

**UNIVERSIDADE FEDERAL DE ALFENAS**

**HERIQUES FRANDINI GATTI**

**THE SBND PHOTON DETECTION SYSTEM ASSEMBLY AND  
INSTALLATION**

**POÇOS DE CALDAS/MG**

**2024**

**HERIQUES FRANDINI GATTI**

**THE SBND PHOTON DETECTION SYSTEM ASSEMBLY AND  
INSTALLATION**

Dissertação apresentada como parte dos requisitos para obtenção do título de Mestre em Física pela Universidade Federal de Alfnas. Área de concentração:Física Aplicada.

Orientador(a): Gustavo do Amaral Valdiviesso

Coorientador(a): Ana Amélia Bergamini Machado

**POÇOS DE CALDAS/MG**

**2024**

Sistema de Bibliotecas da Universidade Federal de Alfenas  
Biblioteca Campus Poços de Caldas

Frandini Gatti, Heriques.

The SBND photon detection system assembly and installation / Heriques  
Frandini Gatti. - Poços de Caldas, MG, 2024.  
70 f. : il. -

Orientador(a): Gustavo do Amaral Valdiviesso.  
Dissertação (Mestrado em Física) - Universidade Federal de Alfenas,  
Poços de Caldas, MG, 2024.  
Bibliografia.

1. Oscilação de neutrinos. 2. Short baseline anomaly. 3. Short-baseline  
near detector (SBND). 4. Fluxo de neutrinos BNB. 5. Sistema de detecção de  
fótons (PDS). I. Valdiviesso, Gustavo do Amaral, orient. II. Título.

**HERIQUES FRANDINI GATTI**


**THE SBND PHOTON DETECTION SYSTEM ASSEMBLY AND  
INSTALLATION**

O(A) Presidente da banca examinadora abaixo assina a aprovação da Dissertação apresentada como parte dos requisitos para obtenção do título de Mestre em Física pela Universidade Federal de Alfenas. Área de concentração: Física Aplicada.

Aprovado em: 22 de maio de 2024

**Dr. Anibal Thiago Bezerra**  
Universidade Federal de Alfenas

**Dr. Vincent Basque**  
Fermi National Accelerator Laboratory

---

**Dr. Gustavo do Amaral Valdiviesso**  
Presidente da Banca Examinadora

**gov.br**

Documento assinado digitalmente  
**GUSTAVO DO AMARAL VALDIVIESSO**  
Data: 23/07/2024 07:48:06-0300  
Verifique em <https://validar.it.gov.br>

POÇOS DE CALDAS/MG  
2024

Este trabalho é dedicado às pessoas que vêm  
diversão na resolução de problemas,  
Motivação em responder uma pergunta,  
Paixão em criar e inovar sem medo de se desafiar  
Ou como conhecidos, cientistas.

## ACKNOWLEDGEMENTS

I would like to express my sincere gratitude to several individuals and institutions who have supported me throughout the journey of completing this dissertation.

First, I am deeply thankful to my supervisors, Dr. Gustavo do Amaral Valdivieso, for the guidance, encouragement, and the many good and great talks throughout the research process. and my co-supervisor, Dra. Ana Amélia Bergamini Machado, whose the guidance, knowledge share and support went beyond academic and professional formalities, becoming a great personal friend.

I would also like to extend my appreciation to the members of the SBND Collaboration, for the friendly and warm welcome while supporting me in Fermilab, also for their valuable feedback and constructive criticism that greatly enhanced the quality of this work

I am grateful to Fermilab for providing resources and facilities essential for conducting research. Especially to technician John Najdzion, whose way of organizing, planning, and executing work has revolutionized my approach to thinking and addressing tasks, in addition to the excellent and inspiring conversations.

I am also indebted to my friends and colleagues for their support, encouragement, and stimulating discussions that have enriched my research experience. With a special thank you to Gabriela Vitti Stenico, Pedro Simoni Pasquini, and Gabriel Botogoske, who became great friends made during this stage, and whose friendship has become of immeasurable value.

Last but not least, I wish to express my heartfelt appreciation to all the participants who generously contributed their time and insights to this study.

Their contributions are deeply appreciated and have significantly enriched the outcome of this research.

This study was financed in part by the Coordenação de Aperfeiçoamento de Pessoal de Nível Superior – Brasil (CAPES) – Finance Code 001.

*“Nature is infinite; both nothing and everything.  
In this way, it has unfathomable power.”*  
(Hatsumi, 2012, p. 29). (1)

## ABSTRACT

Developed under the focus of advancements in experiments contributing to the understanding of Neutrinos, which are one of the least well-known types of particles in the standard model. The Short-Baseline Near Detector (SBND) is one of three Liquid Argon Time Projection Chamber (LArTPC) neutrino detectors positioned along the axis of the Booster Neutrino Beam (BNB) at Fermilab. This detector is equipped with a powerful and innovative Photon Detection System (PDS) designed as a hybrid concept combining a primary system of 120 photomultiplier tubes and a secondary system of 192 X-ARAPUCA devices, all of which are located behind the anode plane. Owing to its complexity, the installation of this system was compelled to satisfy rigorous criteria of quality starting from the construction of the X-ARAPUCA devices, going through all the assemblies and installation procedures, and finishing with the cabling. The work was carried out following many steps, each of which was compelled to fulfill safety, cleanliness, and lightproof requirements (as many of the its devices are sensitive to UV and blue light), and ended successfully, accomplishing the delivery of the system ready for the next steps of detector construction.

**Keywords:** neutrino oscillation; short baseline anomaly; Short-Baseline Near Detector (SBND); BNB neutrino flux; photon detection system (PDS); detector installation.



## RESUMO

Desenvolvido com foco em avanços em experimentos que contribuem para a compreensão dos neutrinos, que são um dos tipos de partículas menos conhecidos no Modelo Padrão. O Short-Baseline Near Detector (SBND) é um dos três detectores de neutrinos de Câmara de Projeção Temporal de Argônio Líquido (Liquid Argon Time Projection Chamber - LArTPC) posicionados ao longo do feixe do Booster Neutrino Beam (BNB) no Fermilab. Este detector é equipado com um Sistema de Detecção de Fótons (Photon Detection System - PDS) poderoso e inovador projetado como um conceito híbrido que combina um sistema primário de 120 tubos fotomultiplicadores e um sistema secundário de 192 dispositivos X-ARAPUCA, todos localizados atrás do plano do anodo. Devido à sua complexidade, a instalação deste sistema foi compelida a satisfazer critérios rigorosos de qualidade, começando pela construção dos dispositivos X-ARAPUCA, passando por todas as etapas de montagem e procedimentos de instalação, e terminando com o cabeamento. O trabalho foi realizado seguindo muitas etapas, cada uma das quais foi compelida a cumprir requisitos de segurança, limpeza e proteção contra luz (Uma vez que muitos componentes são sensíveis a luz UV e azul), e terminou com sucesso, alcançando a entrega do sistema pronto para as próximas etapas da construção do detector.

**Palavras-chave:** oscilação de neutrinos; short Baseline Anomaly; Short-Baseline Near Detector (SBND); fluxo de neutrinos BNB; sistema de Detecção de Fótons (PDS); instalação do detector.

## LIST OF FIGURES

Figure 1 – $W^+$ boson decaying into a massive lepton (electron, muon or tau) and its respective neutrino (2) . . . . .	23
Figure 2 – Excessive neutrinos observed in miniBoone (3) . . . . .	26
Figure 3 – Higgs’ mechanism for the Dirac’s particle (4) . . . . .	27
Figure 4 – Higgs’ mechanism for the Majorana particle (4) . . . . .	28
Figure 5 – Scintillation and ionization mechanism of liquid argon (from (5)). Free excitons and holes are self-trapped within about 1 ps from their production and result into excited, $Ar_2^*$ , or ionized $Ar_2^+$ argon dimers. $Ar_2^+$ recombines with a thermalized electron to form $Ar_2^*$ which in turn decays non-radiatively to the first singlet and triplet (6) . . . . .	33
Figure 6 – Sensitivities at $3\sigma$ (solid red line) and $5\sigma$ (dotted red line) to a light sterile neutrino in the $\nu_\mu \rightarrow \nu_e$ appearance channel (left) and $\nu_\mu \rightarrow \nu_\mu$ disappearance channel (right). For reference, the LSND favored region at 90% C.L. (shaded blue) and 99% C.L. (shaded gray) is shown (7) . The $3\sigma$ global $\nu_e$ appearance allowed region (shaded red) and $\nu_\mu$ disappearance exclusion limit (black line) from Ref. (8) are also plotted, along with the $3\sigma$ global best fit regions (shaded green) from Ref. (9) .	35
Figure 7 – Normalized spectra of $\nu_\mu$ events in SBND, with the absolute number of events expected for $6,6 \times 10^{20}$ POT shown in the legend. The inclusive charged-current (CC) and neutral-current (NC) spectra are shown on the left (not stacked), and the breakdown into CC exclusive channels separated by the number of pions in the final state is shown on the right (stacked). . . . .	35
Figure 8 – Left: Standard ARAPUCA mechanism. The photon enters the box, it is converted by the WLS slab and is captured inside the ARAPUCA. Center: Total internal reflection. A converted photon enters the box and it is converted by the WLS in the slab and trapped by total internal reflection. Right: High angle photons. A photon with high incidence angle inside the box, is trapped in the liquid argon gap between the filter and the acrylic slab. Notice that in this last case the guided photons are not shifted by the slab (10) . . . . .	39
Figure 9 – Left: A Frame of one SBND X-ARAPUCA module as it is assembled Right: An exploded view of the the module showing its internal components (a) dichroic Filter, (b) WLS Guide, (c) Electronic boards.	40
Figure 10 – A view of the internal part of a X-ARAPUCA front G10 frame with the holding screws and the 3D printed covers . . . . .	41

Figure 11 – X-TDB Electronics board with electronics scheme . . . . .	42
Figure 12 – X-ASB Electronics board with electronics scheme . . . . .	42
Figure 13 – A view of two X-Arapucas side by side where it possible to see the one with not coated dichroic filters (left) and the one with coated dichroic filters (right) . . . . .	43
Figure 14 – A view of the WLS plate installed inside a half open X-Arapucas . . . . .	44
Figure 15 – A set of 8x Standoffs and all the M5 screws washers and spacers for mounting one set wit a pair of X-Arapucas. . . . .	45
Figure 16 – The Adapter plate mount for assembling the X-Arapucas (left) and a set of Two X-Arapucas mounted on a Adapter plate (right) where the one of the aluminum spacers are highlighted. . . . .	45
Figure 17 – X-ARAPUCA cover screws . . . . .	47
Figure 18 – Boards protective film of reflective adhesive installation and handling . . . . .	48
Figure 19 – Electronics boards insertion . . . . .	48
Figure 20 – Stress relief bar instalation . . . . .	49
Figure 21 – PMT tube with cover installed . . . . .	51
Figure 22 – PDS box with the wires routed the position inside the box . . . . .	53
Figure 23 – Mock PDS box attached to the lifting bar during the load test . . . . .	54
Figure 24 – Model of the lifting structure mounted in the ATF with an expanded view of the hook attachment . . . . .	57
Figure 25 – The cables being hold in place with the PTFE clamps . . . . .	63
Figure 26 – An internal view of the PDS system installed in the west APA with the back covers in. All X-Arapucas and PMT's can be seen behind the wire planes. . . . .	65
Figure 27 – Views of the PDS cables sitting in tray and routed along the APA . . . . .	66
Figure 28 – The detector with all dark covers during the move procedure . . . . .	67

## LIST OF TABLES

Table 1 – Charges and Masses of the quarks (11) . . . . .	19
Table 2 – Charges and Masses of the leptons (11) . . . . .	19
Table 3 – Charge and Mass of the gauge boson. (11) . . . . .	22

## LIST OF ABBREVIATIONS AND ACRONYMS

ATF	Assembly and Transport Frame
BNB	Booster Neutrino Beam
BooNE	Booster Neutrino Experiment
CC	Charged Current
CPA	Cathode Plane Assembly
CRT	Cathodic Rays Tube
DAQ	Data Acquisition
DUNE	Deep Underground Neutrino Experiment
LArTPC	Liquid Argon Time Projection Chamber
LED	Light Emitting Diode
LSND	Liquid Scintillator Neutrino Detector
NC	Neutral Current
PDS	Photon Detection System
PMT	Photo Multiplier Tube
POT	Protons on Target
PPE	Persona Protective Equipment
SBN	Short-Baseline Neutrino
SBND	Short-Baseline Near Detector
SiPM	Silicon Photo Multiplier
TPB	Tetra-Phenyl-Butadiene
TPC	Time Projection Chamber

VUV	Vacuum Ultra Violet
WLS	Wave Length Shifter
X-ASB	X-Arapuca SiPM Board
X-TDB	X-"Tongue Depressor Board"

## LIST OF SYMBOLS

$e^-$	Electron
$\pi^0$	Neutral Pion
$\pi^+$	Positive Pion
$\pi^-$	Negative Pion
$\mu$	Muon
$\tau$	Tau
$\nu_e$	Electron Neutrino
$\nu_\mu$	Muon Neutrino
$\nu_\tau$	Tau neutrino
Ar	Argon
Quark	u Up
	d Down
	c Charm
	s Strange
	t Top
	b Bottom

# CONTENTS

<b>1</b>	<b>INTRODUCTION</b>	17
1.1	ABOUT THIS TEXT	17
<b>2</b>	<b>INTRODUCTION TO NEUTRINOS PHYSICS</b>	18
2.1	STANDARD MODEL	18
2.2	THE NEUTRINOS	22
2.3	NEUTRINOS OSCILLATION	23
2.4	SHORT BASELINE ANOMALY	25
<b>2.4.1</b>	<b>Sterile Neutrino</b>	26
2.4.1.1	Seesaw Mechanism	27
<b>3</b>	<b>NEUTRINO DETECTION</b>	30
3.1	TIME PROJECTION CHAMBER TPC	30
<b>3.1.1</b>	<b>The Reasons for Using Liquid Argon</b>	31
<b>3.1.2</b>	<b>The Signal Formation</b>	31
<b>3.1.3</b>	<b>The Liquid Argon Scintillation Light Emission</b>	32
<b>4</b>	<b>THE SBND EXPERIMENT</b>	34
4.1	SHORT-BASELINE NEAR DETECTOR (SBND)	34
4.2	SBND PHYSICS PROGRAM	34
<b>4.2.1</b>	<b>Perform a high-precision measurement of the BNB neutrino flux</b>	34
<b>4.2.2</b>	<b>Perform high precision measurements of cross-sections of muon and electron neutrinos on Argon</b>	36
<b>4.2.3</b>	<b>Search for Beyond Standard Model physics</b>	36
<b>4.2.4</b>	<b>Advance further the LArTPC detector technology</b>	36
4.3	SBND CONSTRUCTIVE CHARACTERISTICS	36
<b>4.3.1</b>	<b>TPC - Time Projection Chamber</b>	37
<b>4.3.2</b>	<b>SBND PDS - Photon Detection System</b>	37
<b>5</b>	<b>ASSEMBLY AND INSTALLATION OF THE SBND PDS SYSTEM</b>	38
5.1	THE X-ARAPUCAS	38
<b>5.1.1</b>	<b>Arapucas Structure</b>	39
<b>5.1.2</b>	<b>Clean tent and Working Bench</b>	46
<b>5.1.3</b>	<b>Assembly Procedure</b>	46
<b>5.1.4</b>	<b>Quality control</b>	49
5.2	PHOTON DETECTION BOXES	50
<b>5.2.1</b>	<b>PMT's Assembly in PD-Box</b>	50
<b>5.2.2</b>	<b>Arapucas Assembly in PD-Box</b>	51
<b>5.2.3</b>	<b>Assembly Procedure</b>	51
<b>5.2.4</b>	<b>Wiring and Pre Routing</b>	52



5.2.5	Storage and Protection . . . . .	53
5.2.6	PD-Box Lifting Bar . . . . .	54
5.2.7	Quality Control . . . . .	55
5.3	THE INSTALLATION OVERVIEW . . . . .	56
5.3.1	Hanging structure . . . . .	56
5.3.2	Problems and Concerns . . . . .	57
5.3.3	The covers and protections . . . . .	58
5.3.4	The PDS installation team and functions . . . . .	58
5.3.5	Work Procedure . . . . .	59
5.3.6	The pos installation checkups . . . . .	62
5.3.7	Cabling . . . . .	62
5.3.8	Quality control . . . . .	64
6	FINAL THOUGHTS . . . . .	65
	REFERENCES . . . . .	68

# 1 INTRODUCTION

## 1.1 ABOUT THIS TEXT

This dissertation is divided into three parts. In the first part, you will find an introduction to neutrino physics and a brief discussion about some of the open questions studied in neutrino theory. Also, in the first part, you will find a discussion about neutrino detection techniques with a focus on time projection chambers where the medium is liquid argon.

The second part will present the Short Baseline Near Detector (SBND) with its physics program and constructive characteristics.

The third and last part will show the assembly process of the SBND photon detection system, demonstrating some key components characteristics, some relevant structural parts to the system, and a discussion of the installation criteria and concerns.

Finally, The dissertation will conclude with a report of the installation procedure undertaken and the final checkups.

## 2 INTRODUCTION TO NEUTRINOS PHYSICS

Neutrinos are neutral elementary particles produced via weak interactions by the unstable particle and radioactive element decays. They belong to the lepton class, fermions that do not interact via strong force and- as far as we know- there are three different neutrino types, or “flavors”, each one associated with a charged lepton (12). They were first postulated in 1930 by Wolfgang Pauli to address an explanation to the beta decay energy spectrum (13). In a letter to the Physical Institute of the Federal Institute of Technology, Zurich (14), Pauli proposed that a neutral, very light, and spin-half particle was carrying away the missing energy and angular momentum of the particles in the nuclear reaction. Incorporating Pauli’s neutrino hypothesis, Enrico Fermi formulated in 1934 the mathematical theory of weak interactions, in which a neutron converts into a proton and simultaneously creates an electron and an antineutrino.(15)

Besides successfully predicted the correct shape of the energy spectrum of the emitted electrons in beta decay, Fermi’s theory of the weak force also suggested a reaction by which a free neutrino would interact with matter producing detectable products: the inverse beta decay process. However, due to the interaction’s weak character, neutrino’s first experimental detection occurred twenty-five years later its postulation. In 1956, Reines and Cowan reported in Ref. (16) the preliminary observation of neutrino inverse beta decay reactions in a liquid scintillator detector. “For the detection of the neutrino”, Reines won the Nobel prize in 1995.(15)

The idea of the neutrinos kept evolving in 1962, Leon M. Lederman, Melvin Schwartz, and Jack Steinberger reported the existence of a second neutrino type with the first detection of the muon neutrino ( $(\nu_\mu)$  (17). The tau neutrino detection was announced in the summer of 2000 by the DONUT collaboration at Fermi National Accelerator Laboratory (Fermilab) (17).

In 1957 Bruno Pontecorvo suggested the idea of neutrino masses and oscillations (18) and generalized the oscillation in 1967 (19). The deficit of electron neutrinos coming from the sun was reported by many experiments until being addressed as the neutrino oscillation phenomenon by the Sudbury Neutrino Observatory (SNO). In 2015, Arthur McDonald, the director of SNO, won the Nobel Prize “for the discovery of neutrino oscillations, which shows that neutrinos have mass”. Only in 1998, the Super-Kamiokande experiment detected neutrino oscillations for the first time with great statistical significance.

### 2.1 STANDARD MODEL

The known Universe is made of elemental particles. What we know about them is described by the Standard Model. The SM can explain almost all of the experimental

data which is obtained in the area, and it is one of the most important concepts in physics nowadays. (2)

The standard model list as particles: quarks, leptons, gauge bosons, and the Higgs boson.

The quarks can be found in 6 distinct flavors: up (u), down (d), strange (s), charm (c), top (t) and bottom (b). In the table 1 are shown the masses and the electric charge (in units of  $e$ ). (2)

Table 1 – Charges and Masses of the quarks (11)

Quark	Acronym	Mass	Charge ( $e$ )	Weak Isospin		Weak Hypercharge	
				Left	Right	Left	Right
Up	u	2.16 $MeV$	2/3	1/2	0	1/3	4/3
Down	d	4.67 $MeV$	-1/3	-1/2	0	1/3	-2/3
Charm	c	1.27 $GeV$	2/3	1/2	0	1/3	4/3
e Strange	S	93.4 $MeV$	-1/3	-1/2	0	1/3	-2/3
Top	t	172.69 $GeV$	2/3	1/2	0	1/3	4/3
Bottom	b	4.18 $GeV$	-1/3	-1/2	0	1/3	-2/3

Source: Adapted from Workman (2022). (11)

However the quarks are never found isolated in nature, they are always in bounded states (due to color lockdown, more details in (4)) forming baryons or mesons. The baryons are states formed by 3 quarks, and as an example we have the neutrons and the protons, formed respectively of udd and uud. But the mesons are states formed by two quarks, and as an example, we have the pions ( $\pi^0$ ,  $\pi^+$  and  $\pi^-$ ).

The other particle classification are the leptons. The leptons also are found in 6 distinct flavors, and they are: the muon ( $\mu$ ), the electron ( $e^-$ ), the tau ( $\tau$ ), the muon neutrino ( $\nu_\mu$ ), the electron neutrino ( $\nu_e$ ) and the tau neutrino ( $\nu_\tau$ ). In the table 2 are shown the masses and the electric charge (in units of  $e$ ). (2)

Table 2 – Charges and Masses of the leptons (11)

Lepton		Mass	Charge	Weak Isospin		Weak hypercharge	
				Left	Right	Left	Right
Electron	$e^-$	0.51 $MeV$	-1	-1/2	-1	-2	4/3
Muon	$\mu$	105.66 $MeV$	-1	-1/2	-1	-2	4/3
Tau	$\tau$	1776.86 $MeV$	-1	-1/2	-1	-2	4/3
Electron neutrino	$\nu_e$	< 1.1 $eV$	0	1/2		-1	
Muon neutrino	$\nu_\mu$	< 1.1 $eV$	0	1/2		-1	
Tau neutrino	$\nu_\tau$	< 1.1 $eV$	0	1/2		-1	

Source: Adapted from Workman (2022). (11)

The electron, the muon and the tau have electric charge  $e^-$ , while the neutrinos have a null electric charge. By the standard model, theoretically, the neutrinos should have a mass equal to zero, however, nowadays we know that they must have mass - as will be discussed in [2.3](#).

The gauge bosons are responsible for the fundamental forces known today in nature, in order of magnitude: strong force, electromagnetic force, weak nuclear force and gravitational force, the last one not explained by the Standard Model. They are called bosons because they have an integer spin, different from quarks and leptons that have half spin and therefore are fermions.

The electromagnetic force mediator is the photon, having null mass and charge. Its representation is made through the unitary group (U(1)).

The weak nuclear force however has three mediators and they are:  $W^+$ ,  $W^-$  and the Z. Unlike the photon, they do have mass and, except for Z, they do have charge. They are represented by the special unitary group of degree 2 (SU(2)). The weak nuclear force is the only one that can change the flavor of the particles, being able to make a quark change its flavor to another quark flavor or a lepton change its flavor to another lepton flavor. The area that studies this force is called flavourdynamics.

Another interesting characteristic of this force is that exclusively particles with left-handed chirality and right-handed antiparticles can participate in the charged weak interaction (mediated by the  $W^+$  and  $W^-$  bosons), hence is capable to break the CP symmetry.

The electromagnetic force and the weak nuclear force can be unified in a single force called electroweak force with U(1) X SU(2) gauge symmetry. Due to the break of the electroweak symmetry the four already mentioned gauge bosons, the photon,  $W^+$ ,  $W^-$  and the Z emerged.

The symmetry break of the U(1) part creates the quantum number  $Y_W$ , known as weak hypercharge. The symmetry break of the SU(2) part creates the quantum number  $T_3$ , known as weak isospin. Only particles with  $T_3$  interact by charged weak interactions, therefore, of the elementary particles, only particles with left-handed chirality and antiparticles with right-handed chirality carry a weak isospin different than zero. In contrast, the coupling with the W boson is a linear combination of the weak isospin and the weak hypercharge.

For integrity reasons, the tables [1](#) and [2](#) were added as well columns representing the weak isospin and the weak hypercharge. The table is shown the values of both types of chirality: left-handed chirality (*Left*) and right-handed chirality (*Right*). For the respective antiparticles, you should simply reverse the sign of all values and exchange the columns *Right* and *Left*.

The already discussed symmetry break is responsible for the mass of the weak gauge bosons. Due they have mass, the weak nuclear force has a short range, unlike the electromagnetic force which has an infinity range, since the photon has its mass equal to zero.

The carrier of the strong force are the gluons and they are described by the SU(3) gauge's theory. Because of that symmetry, there are three types of force "charge", which are the colours, and they are named red, green and blue. Hence this area of Physics is called chromodynamics.

Quarks have a linear combination of those colours and anti-quarks have a linear combination of the anti-colours (they are anti-red, anti-green and anti-blue). However, because of the colour lockdown, the sum total must be equal to zero - that means that the final colour of the particle has to be "white". For mesons - there are formed by two quarks - one of the particles must be the anti-colour of the other, in other words, if one of the particles is red, the other particle must be anti-red. For baryons - there are formed by three quarks - every one of the particles must have distinct colors in such a way that the "combination" of those colours is white. The gluons however only couple particles with colour charge different from zero.

The gluons are the exception and don't have to be white, in fact gluons show two colour charges at the same time: one normal colour and one anti-colour. Is to be expected that there are nine distinct types of gluons, once there are three colours and three anti-colours, however there are only eight SU(3) group generators, and therefore only eight type of gluons. However, due to colour lockdown, the gluons are confined only to the surroundings of the quarks. So even though the gluons don't have mass, the strong force does not have an infinity range.

The leptons do not have colour charge, and therefore do not participate in strong force. This is main difference between quarks and leptons.

The four gauge bosons of the electroweak force plus the eight gluons have spin equal to one. The only gauge boson that was not discovered yet is the graviton, responsible for the gravitational force and it's not really a part of the Standard Model. It is expected that its mass is equal to zero, once the gravitational force has an infinity range. Its also expected that the has spin equal to two, once its source is the energy-momentum tensor. The gravity is the weakest one of the four fundamental forces.

In the table 3 is shown the gauge boson characteristics.

Table 3 – Charge and Mass of the gauge boson. (11)

Gauge boson	Spin	Mass	Charge( $e$ )	Weak isospin	Weak hypercharge
Photon	1	0 eV	0	0	-0
$W^+$	1	80.34 GeV	1	+1	0
$W^-$	1	80.34 GeV	-1	-1	0
Z	1	91.19 GeV	0	0	0
Gluon	1	0 eV	0	0	0
Graviton	2	0 eV	0	0	0

Source: Adapted from Workman (2022). (11)

Finally, we have the Higgs boson that is a substantial piece of the standard model and the last one of them to be discovered - at least at this moment. The Higgs boson is a particle with a spin equal to zero, and its interaction with the standard model's fundamental particles generates the masses of those. Furthermore, it is responsible for the electroweak symmetry break that was explained earlier.(2)

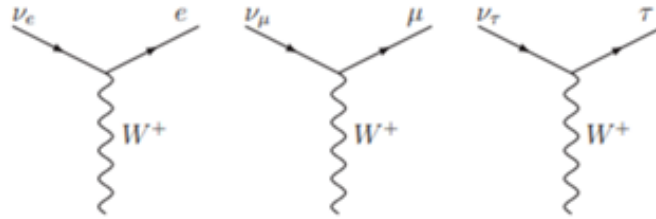
## 2.2 THE NEUTRINOS

Neutrinos hold the second-highest abundance among particles within the Standard Model, yielding only to photons and, however, the most difficult to detect. As explained in 2.1 the reason behind that is because the neutrino does not interact with the strong force and - because of its neutral charge - it does not interact with the electromagnetic force. The neutrino interacts only with the gravitational and the weak force, however - due to the fact that its mass is too small - its interaction with the gravitational force is weak. Therefore its only effective interaction with the rest of the universe is the weak nuclear force.

The neutrinos exist in three different flavours: The electron neutrino, the muon neutrino and the tau neutrino. The names are based on how they are created from a weak charged current. For instance, if a neutrino is created with an electron in weak interaction, this neutrino will be called an electron neutrino. If it's created with a muon, it'll be called an muon neutrino and the same logic works with the tau neutrino. In the figure 1 it is shown each one of the given examples.

This happens because a quantity called leptonic number is conserved. There are three types of lepton number: the muon lepton number, the electron lepton number and the tau lepton number. As an example, the electron and the electron neutrino carry value +1 in its electron number and 0 in the other two numbers. The antiparticles, however, carry the opposite value, for instance, the positron carries the value -1 in its electron

Figure 1 –  $W^+$  boson decaying into a massive lepton (electron, muon or tau) and its respective neutrino (2)



Source: Botogoske (2023, p.28). (2)

number. However, it is necessary to notice that the number is usually conserved - which will be explained in 2.3.

Another important characteristic of the neutrinos is that they always have left-handed chirality and helicity, and the antineutrinos have right-handed chirality and helicity.

The helicity is a projection of the spin in the movement direction and it is a movement constant. The chirality is more abstract, but represents how it transforms in Poincare's representation, and it is a Lorentz invariant. In the massless regime, both of them represent the same thing. Therefore, if the neutrino has no mass it would be coherent to find only neutrinos with the same chirality and helicity, however, since the neutrino has mass, it is expected that its chirality evolves in time.

Neutrinos have a lot of other open questions. Today physics knows that neutrinos have mass, but don't know their mass of them. It's only known that they are the lightest standard model particle (with exception of the photon). By the fact they have mass, neutrinos oscillate between their flavor states but we don't know if neutrinos and anti-neutrinos oscillate differently (CP violation in leptonic sector). The order of mass hierarchy isn't now today and as a consequence isn't known which neutrinos' mass is heavier. Also isn't known if neutrinos are Dirac particles or Majorana particles, and if exist other types of neutrinos and interactions. Neutrinos can also be candidates to be dark matter.

### 2.3 NEUTRINOS OSCILLATION

Intending to measure the solar neutrino flux, the Homestake (20) experiment was designed. In this experiment, was expected a neutrino interaction ratio of 1.7 per day and only 0.48 per day were being detected. This was the first evidence that something was missing in the Physic theory of neutrinos.(2)

The anomalous result persisted, in the Super-kamiokande experiment that utilizes the Cherenkov radiation measured 0,465 of the expected flux of electron neutrinos



originating from the Sun.

One of the hypotheses for this problem is that the electron neutrino, during the path from the Sun to the Earth, was changing into two different flavors: the tau and the muon flavor. Since the neutrino has mass, it was shown in (19) that could exist the possibility of the neutrinos oscillating between flavors.

To determine whether, in fact, the neutrinos were changing flavors, the experiment Sudbury Neutrino Observatory (SNO) was designed (21). In this experiment were measured, individually, the three types of neutrinos arriving on the Earth. The expected electron neutrino flux was to be  $(5, 1_{-0.81}^{+1.01}).10^{-6} cm^{-2}.s^{-1}$ .

The measured flux is shown in 1.

$$\begin{aligned}\phi(\nu_e) &= (1, 76 \pm 0, 14).10^{-6} cm^{-2}.s^{-1} \\ \phi(\nu_\mu + \nu_\tau) &= (3.41_{-0.90}^{+0.93}).10^{-6} cm^{-2}.s^{-1}\end{aligned}\tag{1}$$

Therefore, the total flux which it's the sum of both fluxes that is equal to  $(5, 09_{-0.86}^{+0.90}).10^{-6} cm^{-2}.s^{-1}$  (21), which is consistent with the solar model.

There were two choices: accept that the solar model was mistaken and the Sun can produce others neutrino flavors, or assume that the electron neutrinos change into other flavors, this way changing the known Standard model. In fact, the second option was right and, in 2015, both experiments - SNO and the Super-Kamiokande - won the Nobel prize.

The neutrinos, as shown in 2.2, can be classified by their flavors. In quantum mechanics, they can be described in terms of their basis of flavour  $|\nu_e\rangle, |\nu_\mu\rangle$  and  $|\nu_\tau\rangle$ .

The neutrino has mass, however differently of its expected that each flavour neutrino has a well-defined mass value, in fact each neutrino flavour is a linear combination of three distinct mass states,  $|\nu_1\rangle, |\nu_2\rangle$  and  $|\nu_3\rangle$ . Each state of mass has a different mass called  $m_1$ ,  $m_2$  and  $m_3$  respectively. This linear combination is described in 2.

$$\begin{pmatrix} \nu_e \\ \nu_\mu \\ \nu_\tau \end{pmatrix} = \begin{pmatrix} U_{e1} & U_{e2} & U_{e3} \\ U_{\mu1} & U_{\mu2} & U_{\mu3} \\ U_{\tau1} & U_{\tau2} & U_{\tau3} \end{pmatrix} \begin{pmatrix} \nu_1 \\ \nu_2 \\ \nu_3 \end{pmatrix}\tag{2}$$

The 3x3 unity matrix described in the equation 2 is called Pontecorvo–Maki–Nakagawa–Sakata (PMNS) matrix. If each neutrino flavour has a well-defined mass value the matrix should be the identity matrix, however, this does not occur.

The probability for an electron neutrino oscillates to another flavor is given by equation 3, where E is the neutrino energy and L is the distance traveled by the electron neutrino.

$$\begin{aligned}
P(\nu_e \longrightarrow \nu_k)(L) = & \delta_{ek} - 4\text{Re}\left(\sum_{j>i}^{3,3} U_{kj}^* U_{ej} U_{ki}^* U_{ei} \sin^2\left(\frac{m_j^2 - m_i^2}{4E} L\right)\right) \\
& + 2\text{Im}\left(\sum_{j>i}^{3,3} U_{kj}^* U_{ej} U_{ki}^* U_{ei} \left(\sin\left(\frac{m_j^2 - m_i^2}{2E} L\right)\right)\right)
\end{aligned} \tag{3}$$

Therefore the three fundamental wave numbers of oscillation are given by the equation 4(not in natural units).

$$k_{ji} = \frac{c^3(m_j^2 - m_i^2)}{4E\hbar} \tag{4}$$

This way, we conclude that the oscillations between flavors depend on the difference in the square of the masses. Oscillation experiments fix L and E to measure the free parameters.

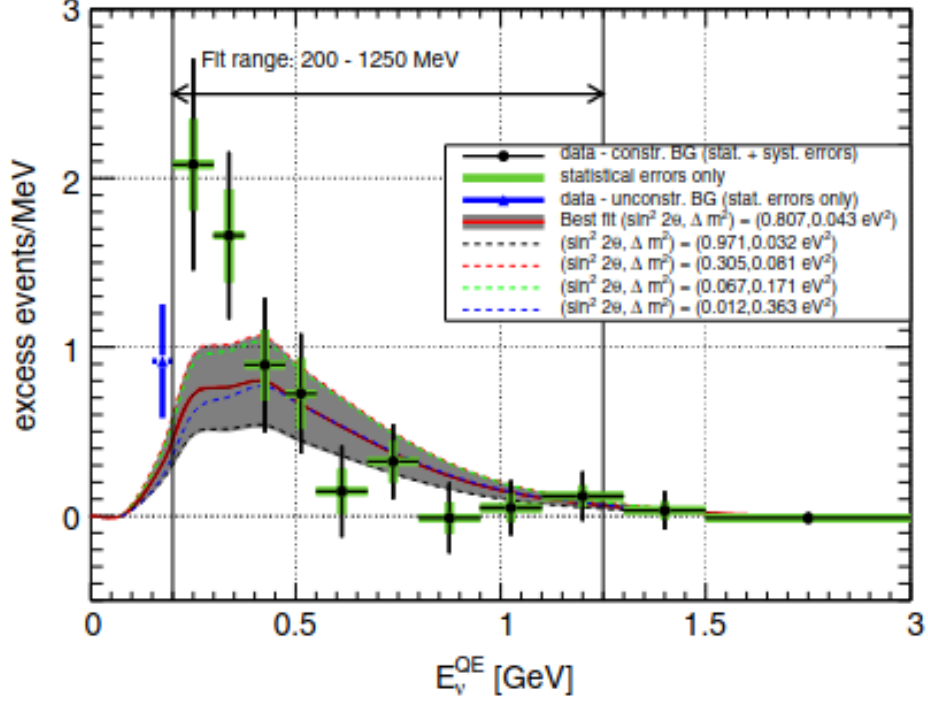
## 2.4 SHORT BASELINE ANOMALY

The Liquid Scintillator Neutrino Detector (LSND) experiment detected an anomaly not predicted by the theory explained in 2.3. The detector, which was placed 30 meters away from the origin of the neutrinos beam, detected an excess of electron neutrinos (22).

Then, the miniBoone experiment also detected anomalies in neutrinos oscillation. The detector was 540 meters away from the origin of the neutrinos beam. The experiment detected an excess of 638 electron neutrinos (3).

In the figure 2 it is shown the excessive electron neutrinos in function of the neutrino energy. The black points are the obtained data with their respective error bars. In the dashed line are the fitted curves for the possibles values of  $\sin^2 2\theta$  and  $\Delta m^2$  - which will be explained in 2.4.1.

Figure 2 – Excessive neutrinos observed in miniBoone (3)



Source: Aguilar-Arevalo (2021, p.19). (3)

One of the possible explanations for the already explained anomaly is the existence of a fourth neutrino flavour, called the sterile neutrino. This neutrino would have no charge, no weak isospin and no weak hypercharge. In other words, they don't interact either with electromagnetic force or with strong and weak force (once they are leptons).

### 2.4.1 Sterile Neutrino

Considering this new flavour, the oscillation model 2 must be modified, adding the new flavour and a new state of mass, as shown in equation 5.

$$\begin{pmatrix} \nu_e \\ \nu_\mu \\ \nu_\tau \\ \nu_s \end{pmatrix} = \begin{pmatrix} U_{e1} & U_{e2} & U_{e3} & U_{e4} \\ U_{\mu1} & U_{\mu2} & U_{\mu3} & U_{\mu4} \\ U_{\tau1} & U_{\tau2} & U_{\tau3} & U_{\tau4} \\ U_{s1} & U_{s2} & U_{s3} & U_{s4} \end{pmatrix} \begin{pmatrix} \nu_1 \\ \nu_2 \\ \nu_3 \\ \nu_4 \end{pmatrix} \quad (5)$$

It is possible to calculate the probability of a flavour change into another. This probability is given by 6 in the short-range limit (15).

$$\begin{aligned} P(\nu_\alpha \longrightarrow \nu_\beta)(L) &= \sin^2(2\theta_{\alpha\beta}) \sin^2\left(\frac{\Delta m_{41}^2 L}{4E}\right) \\ P(\nu_\alpha \longrightarrow \nu_\alpha)(L) &= 1 - \sin^2(2\theta_{\alpha\alpha}) \sin^2\left(\frac{\Delta m_{41}^2 L}{4E}\right) \end{aligned} \quad (6)$$

In which the terms  $\sin^2 2\theta_{\alpha\beta}$  are the functions of  $U_{\alpha 4}$  and  $U_{\beta 4}$  and the terms used in figure 2 to fit the curve are the  $\Delta m_{41}^2$  and the term  $\sin^2 2\theta_{\mu e}$ .

#### 2.4.1.1 Seesaw Mechanism

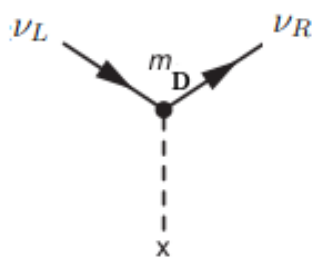
This section will explain one of the possible origin of the normal and sterile neutrino masses, the seesaw mechanism.

The mass acquisition mechanism through the Higgs Bosons requires the existence of both chiralities. We could assume the existence of both chiralities for neutrinos and the Lagrangian of the neutrinos can be describe as in 7.

$$\mathcal{L}_D = -m_D(\bar{\nu}_R\nu_L + \bar{\nu}_L\nu_R) \quad (7)$$

This is equals to the following interaction, shown in the Feynman's diagram of the figure 3.

Figure 3 – Higgs' mechanism for the Dirac's particle (4)



Source: Adapted from Thomson (2013). (4)

However if that is, in fact, the origin of the neutrino's mass, it is expected to have a mass in the same order of magnitude of the others elemental particles.

Another neutrino mass acquisition form, since it does not have charge, it is through the following Lagrangian 8, without breaking the gauge invariance required to the Standard model.

$$\mathcal{L}_M = -\frac{m_M}{2}((\bar{\nu}^C)_L\nu_R + \bar{\nu}_R(\nu^C)_L) \quad (8)$$

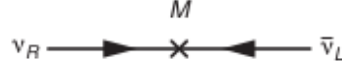
The C index is the CP operator that causes the change of charge and reverses the chirality. In other words,  $(\Psi_{L,R})^C = \Psi^C_{R,L}$ . Therefore is the operator that changes the particle for its antiparticle with the reversed chirality. Hence the equation 8 can be

described as 9.

$$\mathcal{L}_M = -\frac{m_M}{2}((\nu_R^-)^C)\nu_R + \bar{\nu}_R\nu_R^C \quad (9)$$

This mechanism, in theory, is possible for the neutrino, because - since it does not have charge - the coupling of particle and antiparticle - as shown in 4 - does not violate the conservation of the electric charge.

Figure 4 – Higgs' mechanism for the Majorana particle (4)



Source: Adapted from Thomson (2013). (4)

Particles that acquire mass for this model are called Majorana particles, and that imposes the nonexistence of a distinction between the particle and its antiparticle. In other words, the particle is its own antiparticle.

The mechanism that expects neutrinos to have mass is a combination of the mechanism already mentioned: Dirac and Majorana. The Lagrangian becomes 10.

$$\mathcal{L}_{DM} = -m_D\bar{\nu}_L\nu_R - \frac{m_R}{2}(\nu_R^-)^C\nu_R - \frac{m_L}{2}\bar{\nu}_L(\nu_L)^C + h.c. \quad (10)$$

The first term is the coupling of the left-handed chirality neutrino with the right-handed chirality neutrino, generating the Dirac mass ( $m_D$ ). The second term is the coupling of a left-handed chirality antineutrino with a right-handed chirality antineutrino, generating the Majorana mass ( $m_R$ ). The last term is the coupling of a left-handed neutrino with a right-handed neutrino, generating the Majorana mass ( $m_L$ ).

Writing in matrix form the equation 10 it is obtained the equation 11, remembering that  $\bar{\nu}_L\nu_R = \bar{\nu}_R^C\nu_L^C$ , due to the condition of the Majorana.

$$\mathcal{L} = -\frac{1}{2}(\bar{\nu}_L \quad (\nu_R^-)^C) \begin{pmatrix} m_L & m_D \\ m_D & m_R \end{pmatrix} \begin{pmatrix} (\nu_L)^C \\ \nu_R \end{pmatrix} + h.c. \quad (11)$$

When diagonalizing the matrix we got the eigenvalues of the masses described by the equation 12.

$$m, M = \frac{m_R + m_L}{2} \pm \sqrt{\left(\frac{m_R - m_L}{2}\right)^2 + m_D^2} \quad (12)$$

Equaling the term  $m_L$  to zero, once the standard model does not allow this term because it breaks the expected symmetries (23), and also assuming that  $m_R$  is way bigger than  $m_D$ , we got the following mass values shown in 13.

$$\begin{aligned}
 m &\approx \frac{m_D^2}{m_R} \\
 M &\approx m_R
 \end{aligned}
 \tag{13}$$

In other words, for each flavour exists a very small mass that is associated to with a active left-handed chirality neutrino and a much bigger mass that is associated to a right-handed chirality neutrino, that is the sterile neutrino. (2)

### 3 NEUTRINO DETECTION

As previously mentioned, neutrinos do not interact electromagnetically and by strong nuclear forces, so the detection becomes possible by weak nuclear interaction processes with the electrons, nucleons, or whole nuclei of the a detector material (depending on neutrino flavor and energy as well as detector materials, different detection reactions become accessible) (24). Charged particles generated when a neutrino interacts, creating a signature track, flash of light, line of bubbles, change in temperature, or other indicator, depending on the material. Because neutrinos interact so rarely, detectors need to have large volumes and long exposition in order to have good statistics. Also it is needed to shield the detectors for other particles which the interactions could clutter up neutrino data.(25)

Neutrino interaction cross sections rise with the neutrino energy; however, neutrino fluxes from the observable natural sources decrease even more steeply. Hence, expected detection rates decrease as well: While solar neutrinos can be observed with rates of one interaction per day and ton of detector material (already requiring large detectors to acquire meaningful statistics) the high-energy neutrino telescope IceCube employs a billion tons of ice to detect a handful of cosmic neutrinos per year (24) .

Not only the rates, but also the required detector performance, i.e., event reconstruction capabilities, widely defer for the different energy ranges. low-energy (MeV) neutrino events produce virtually point-like interactions. Hence, detectors are optimized to reconstruct position, energy, and (in case of Cherenkov detectors) direction of the final state lepton. At PeV ( $10^{15}$  eV) energies, huge detection volumes on the scale of cubic kilometers are required to detect the minute neutrino fluxes; however, the demand on instrumentation density is very limited: tracks of muons produced in charged-current interactions can easily reach lengths of several hundred meters at such energies. The intermediate energy regime centered on GeV energies is usually considered the most challenging for reconstruction, as interactions on the nuclei of the target atoms can be due to both charged and neutral weak currents and may thus produce relevant amounts of secondary particles, muddling the results of both energy and directional reconstruction algorithms (24) .

#### 3.1 TIME PROJECTION CHAMBER TPC

Although there are other techniques, we will focus on the time projection chamber (TPC) technique, more specifically when the interaction medium is liquefied Argon, forming a LArTPC (liquid Argon Time Projection Chamber). The Time Projection Chamber is the only electronically read gaseous detector delivering direct three-dimensional track information: for each point on the track, x-,y- and z-coordinates are measured

simultaneously. This is of particular importance for pattern recognition in high multiplicity events. The combination of powerful tracking with particle identification capacity over a wide momentum range, based on multiple measurements of ionization loss, is the trademark of the TPC.(26)

The work principle of a LArTPC was described by C. Rubbia (27) based on the works of Nygrem (28) and Charpak (29) . The idea of a TPC consists of a drifting the whole electron image of an event occurring in a noble gas towards a collecting multielectrode array which is then capable of reconstructing the three-dimensional image (x,y,z) of the event from the (x,y) information and the drift time (t). Rubbia propose to extend this concept to a detector where the active medium is a liquefied noble gas (Liquid Argon) giving it the name of LArTPC (liquid Argon Time Projection Chamber).

### 3.1.1 The Reasons for Using Liquid Argon

In addition to being easier to obtain and less expensive when compared to other noble gases, there are several reasons for using liquid Argon as interaction medium for detectors, some of them are: (27)

- High density  $1,4 \text{ g/cm}^3$  (27);
- There is no electron affinity allowing long drift-time;
- High electron mobility (30);
- Is easy to purify and reach high levels of purity;
- It is inert;
- Excellent optical properties;

### 3.1.2 The Signal Formation

As mentioned before the traveling neutrino interact with the Argon nuclei by weak nuclear interaction processes so electron-ion pairs ( $e^-$ ,  $Ar^+$ ) are produced from energy loss by charged particles in liquid argon through the ionization process: (31)

$$N_i = \frac{\Delta E}{W_{ion}}, \quad (14)$$

where  $N_i$  is the number of electron-ion pairs,  $\Delta E$  is the energy loss, and  $W_{ion} = 23.6 \pm 0.3 \text{ eV}$ (32) is the ionization work function.



Some of the ionization electrons are recombined with surrounding molecular argon ions to form the excimer  $Ar_2^*$ . The excimers from both argon excitation and electron-ion recombination undergo dissociative decay to their ground state by emitting a vacuum ultraviolet photon. The free electrons that escape electron-ion recombination are drifted towards the wire planes under the electric field. The wire signals is amplified by a preamplifier and then digitized by an analog-to-digital converter(ADC).

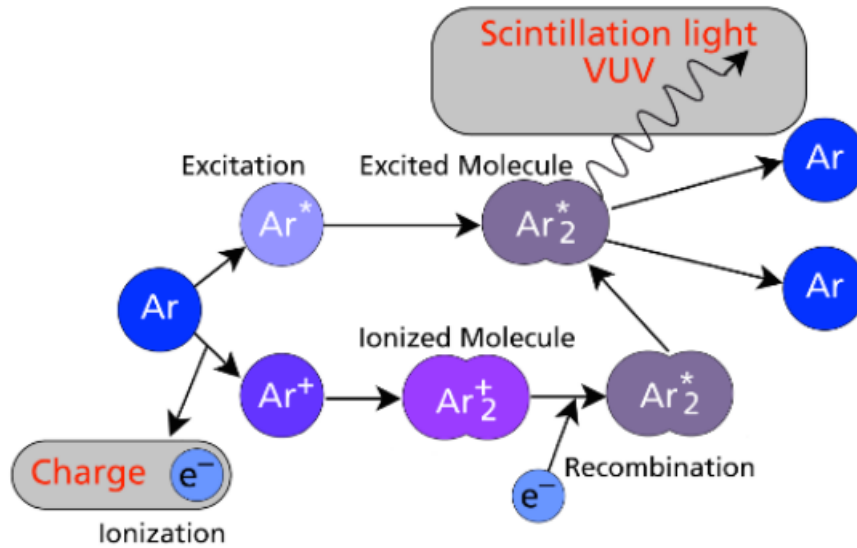
Several effects can affect the electron drift. The electrons can be attached to contaminants in the liquid argon such as oxygen and water, which causes an attenuation of the signal on the TPC wires. The electron cloud is smeared both in the longitudinal and transverse directions by the diffusion effect. For a LArTPC located on the surface, there is a large flux of cosmic ray muons in the detector volume. Because of this, there is a significant accumulation of slow-moving argon ions (space charge) inside the detector, which leads to a position-dependent distortion to the electric field. The distorted electric field changes the electron-ion recombination rate and the trajectory of the free drifting electrons.(31)

### 3.1.3 The Liquid Argon Scintillation Light Emission

As mentioned before the passage of ionizing particles in LAr produces free excitons and electron-hole pairs, the recombination of those ionized molecular argon with some electrons produce the Liquid argon scintillation photons that are emitted in a narrow band of 10 nm centered around 127nm and with a characteristic time profile made by two components originated by the decay of the lowest lying singlet,  $^1\Sigma_u^+$ , and triplet states,  $^3\Sigma_u^+$ , of the excimer  $Ar_2^*$  to the dissociative ground state (6) (as seem in figure 5).

These two states, whose dis-excitation leads to the emission of the scintillation photons, have approximately the same energy with respect to the dissociative ground state, while the lifetimes are very different: in the nanosecond range for  $^1\Sigma_u^+$  and in the microsecond range for  $^3\Sigma_u^+$ .

Figure 5 – Scintillation and ionization mechanism of liquid argon (from (5)). Free excitons and holes are self-trapped within about 1 ps from their production and result into excited,  $Ar_2^*$ , or ionized  $Ar_2^+$  argon dimers.  $Ar_2^+$  recombines with a thermalized electron to form  $Ar_2^*$  which in turn decays non-radiatively to the first singlet and triplet (6)



Source: Araujo (2019, p.11). (5)

The emitted light can be detected using photomultiplier tubes (PMT) or the innovative X-ARAPUCAS combined with some wavelength shifting to convert the VUV light to a detectable wavelength (e.g. the TetraPhenyl Bultadiene (TPB) that absorbs the VUV scintillation light and re-emits around 430nm). The light signal is used to determine the  $T_0$  (time zero when the event occurs) and also can significantly improve the performance of the TPC in terms of energy resolution and particle discrimination. (33)

## 4 THE SBND EXPERIMENT

### 4.1 SHORT-BASELINE NEAR DETECTOR (SBND)

The Short-Baseline Near Detector (SBND) will be one of three liquid argon time projection chamber (TPC) neutrino detectors positioned along the axis of the Booster Neutrino Beam at Fermilab, as part of the Short-Baseline Neutrino (SBN) Program. SBND is characterized by superb imaging capabilities and will record over a million neutrino interactions per year. Thanks to its unique combination of measurement resolution and statistics, SBND will carry out a rich program of neutrino interaction measurements and novel searches for physics beyond the Standard Model. It will enable the potential of the overall SBN sterile neutrino program by performing a precise characterization of the unoscillated event rate, and by constraining BNB flux and neutrino-argon cross-section systematic uncertainties. (34)

### 4.2 SBND PHYSICS PROGRAM

The physics program of SBND consists of four primary science goals:

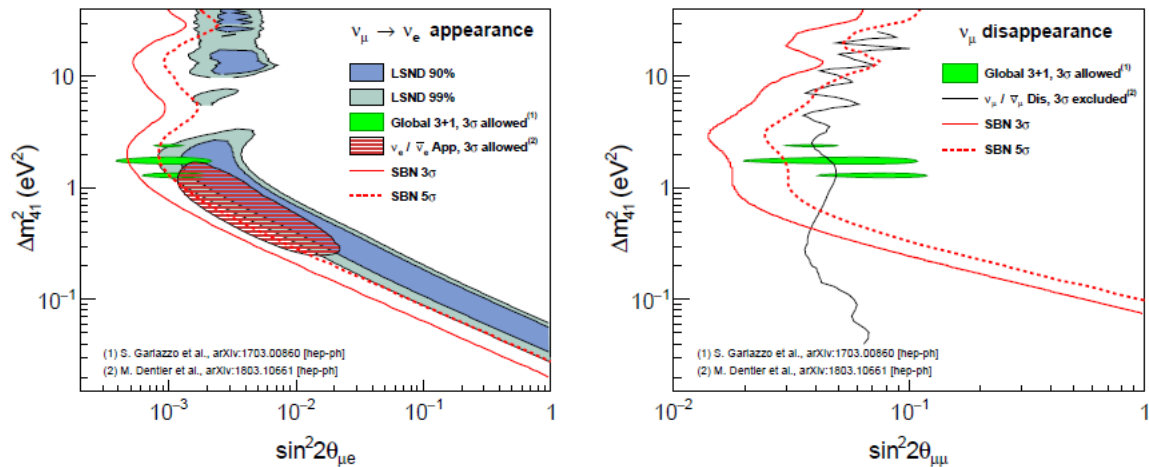
#### 4.2.1 Perform a high-precision measurement of the BNB neutrino flux

The close location of SBND to the beam origin enables the precise measurement of the BNB neutrino flux before any significant oscillation occurs. Due to the high correlation between the measurements of the SBN near and far detectors, a reduction on the systematic uncertainties related to the neutrino flux and the neutrino-argon cross section is achieved. This translates into a boost in the sensitivity to oscillations.

For the  $\nu_e$  appearance oscillation search, SBND will measure the intrinsic  $\nu_e$  component of the BNB flux with large statistics before any oscillation effects. ICARUS and MicroBooNE will search for an excess of  $\nu_e$  in the beam using the SBND measurement as reference. Figure 6 shows the projected sensitivity to oscillations in the squared-mass difference and mixing angle parameter space, which covers the LSND-favored region at  $5\sigma$ .

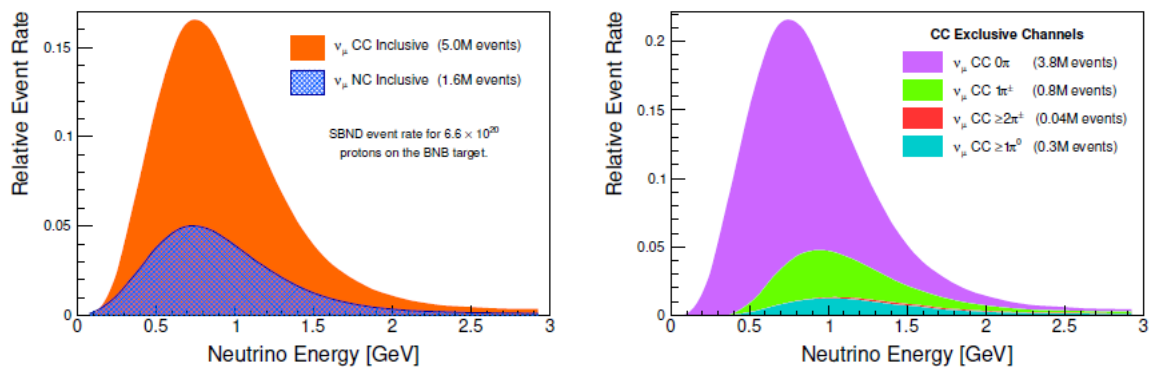
Any observation of oscillation-driven  $\nu_e$  appearance must be accompanied by  $\nu_\mu$  disappearance since the  $U_{\mu 4}$  matrix element appears in both  $\sin^2 2\theta_{\mu e} \equiv 4|U_{\mu 4}U_{e 4}|^2$  and  $\sin^2 2\theta_{\mu\mu} \equiv 4|U_{\mu 4}|^2(1 - |U_{e 4}|^2)$  mixing angle definitions. In the  $\nu_\mu$  disappearance search, SBND will measure the unoscillated  $\nu_\mu$  flux and ICARUS and MicroBooNE will search for the deficit of  $\nu_\mu$ , which is only possible due to the reduction of the flux normalization systematic uncertainty brought by SBND. As shown in figure 6, SBN covers almost completely the global allowed region with  $5\sigma$ .

Figure 6 – Sensitivities at  $3\sigma$  (solid red line) and  $5\sigma$  (dotted red line) to a light sterile neutrino in the  $\nu_\mu \rightarrow \nu_e$  appearance channel (left) and  $\nu_\mu \rightarrow \nu_\mu$  disappearance channel (right). For reference, the LSND favored region at 90% C.L. (shaded blue) and 99% C.L. (shaded gray) is shown (7). The  $3\sigma$  global  $\nu_e$  appearance allowed region (shaded red) and  $\nu_\mu$  disappearance exclusion limit (black line) from Ref. (8) are also plotted, along with the  $3\sigma$  global best fit regions (shaded green) from Ref. (9).



Source: Machado *et al.* (2018, p.16). (35)

Figure 7 – Normalized spectra of  $\nu_\mu$  events in SBND, with the absolute number of events expected for  $6.6 \times 10^{20}$  POT shown in the legend. The inclusive charged-current (CC) and neutral-current (NC) spectra are shown on the left (not stacked), and the breakdown into CC exclusive channels separated by the number of pions in the final state is shown on the right (stacked).



Source: Machado *et al.* (2018, p.18). (35)

### 4.2.2 Perform high precision measurements of cross-sections of muon and electron neutrinos on Argon

SBND will accumulate the largest statistics of neutrino-argon interactions ever recorded. Figure 7 shows the expected number of  $\nu_\mu$  events  $6,6 \times 10^{20}$  protons on target (POT)  $\nu_e$  events per year are expected. This will allow us to discriminate between nuclear models, tune the Monte Carlo event generators and reduce the systematic uncertainties on the oscillation search.

The lessons learned will be useful for the DUNE long-baseline neutrino oscillation physics (36) as well, as the BNB neutrino flux spectrum maximum sits close to the neutrino energy of the second oscillation maximum for DUNE (0.8 GeV) and encompasses a significant number of interactions up to the first DUNE oscillation maximum (2.6 GeV).

### 4.2.3 Search for Beyond Standard Model physics

The close location of SBND to the BNB origin enables searches for Beyond Standard Model particles produced in the beam: dark neutrino portals that explain the MiniBooNE excess (37, 38), heavy neutral leptons that explain the neutrino mass scale (38), light dark matter (39), millicharged particles [(40)]...

A promising idea being developed is the SBND-PRISM concept: the proximity to the beam origin also enables the study of the flux off-axis dependence. The muon neutrino flux and mean energy exhibit a dependence on the angle. On the other hand, electron neutrino distributions are approximately constant. This opens the way for additional handles for background rejection, interaction model constraints, and flux systematic uncertainty reduction.

### 4.2.4 Advance further the LArTPC detector technology

SBND capitalizes on the experience from the previous LArTPC detectors and will expand that experience in terms of detector construction, installation and operation, also testing specific technology of interest for DUNE such as the membrane cryostat or some elements of the photon detection system described next. In addition, the detector simulation, event reconstruction software and data analysis techniques developed for SBND are readily useful for current and future LArTPC detectors.

## 4.3 SBND CONSTRUCTIVE CHARACTERISTICS

SBND consists of a TPC, a photon detection system (PDS) (see figure 3) a cosmic-ray tagger (CRT) . Each subsystem is described in more detail in the following.

### 4.3.1 TPC - Time Projection Chamber

The TPC is 5 m long (in the beam direction), 4 m wide and 4 m tall. A Cathode Plane Assembly (CPA) in the middle of the TPC splits it into 2 drift volumes, each one with a maximum drift length of 2 m. The CPA is biased at -100 KV, resulting in a drift field of 500 V/cm and a drift time of 1,28ms per drift volume. On both sides, Anode Plane Assemblies (APA) with 3 wire planes each are erected to detect the ionization charge and reconstruct the 3-D interaction. The ionization electrons encounter first two induction planes with wires at  $\pm 60^\circ$  from the vertical and are ultimately captured by one collection plane with vertical wires. The wire pitch is 3 mm for all planes as is the plane spacing. This results in 11264 readout channels that are digitized in the liquid argon by cold electronics at 2 MS/s. In addition, a UV laser calibration system is installed within the TPC, capable of creating artificial ionization tracks to characterize the electric field.

### 4.3.2 SBND PDS - Photon Detection System

The PDS consists of two types of photon detectors: photomultiplier tubes (PMTs) and X-ARAPUCAs, a photon-trap that uses silicon photomultipliers (SiPMs) as active devices [14]. An array of 120 8-inch Hamamatsu R5912-mod Cryogenic PMTs is mounted behind the APAs. Among these PMTs, 96 are coated with tetra-phenyl-butadiene (TPB) wavelength shifter to detect scintillation VUV light and 24 are left uncoated to detect only visible light. All PMTs are read out by CAEN ash-ADC electronics digitizing at 500 MHz. The 192 X-ARAPUCAs are installed between the PMTs in modules shown in Figure 3, with half of the X-ARAPUCAs being only sensitive to visible light. In addition, wavelength-shifting reflector foils are installed on the CPA to improve light detection uniformity along the drift direction.

## 5 ASSEMBLY AND INSTALLATION OF THE SBND PDS SYSTEM

### 5.1 THE X-ARAPUCAS

The X-ARAPUCA is an improved version of the ARAPUCA concept (41) which is being considered as one of the possible alternatives for LAr scintillation light detection, but The X-ARAPUCA is not only a development and an optimization of the traditional ARAPUCA one, it is conceived as a mutation of the original idea being a hybrid solution between an ARAPUCA (41) and a light guide (42). and it represents a new perspective for the photon detection system of a LArTPC, which is a technique that allows to perform an accurate 3-D and calorimetric reconstruction of the ionizing events that happen inside its active volume. LAr is known to be an abundant scintillator, emitting about 40 photons/keV of energy deposited by minimum ionizing particles, in absence of electric fields. The light is emitted in the Vacuum Ultra Violet (VUV) region of the electromagnetic spectrum in a 10 nanometers band centered around 127 nm (43). This makes detection harder, since usual (cryogenic) photo-sensitive devices with glass or fused silica windows are insensitive to these wavelengths. The current paradigm for LAr scintillation light detection foresees the use of wavelength shifting (WLS) compounds which absorb VUV light and re-emits it in the visible, where it is easier detectable.(10)

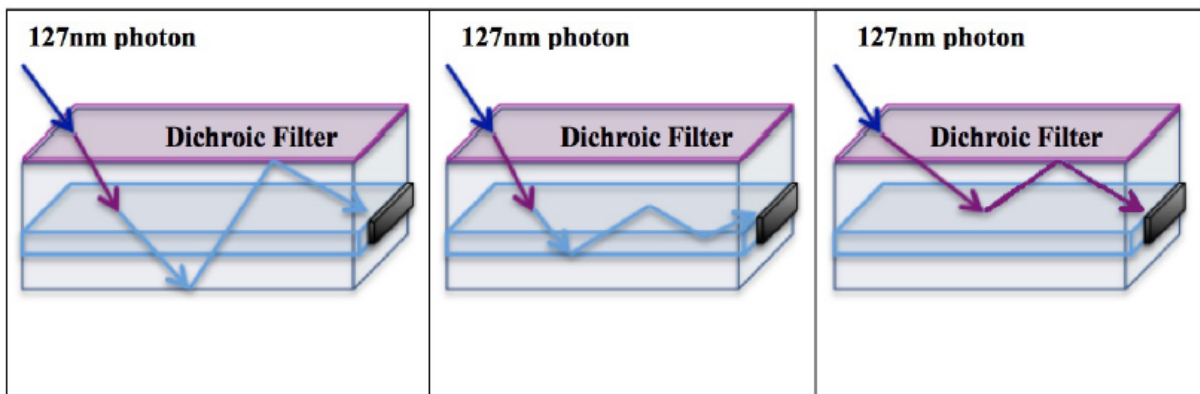
A standard ARAPUCA consists of a box with highly reactive internal surfaces and acceptance windows constituted by a short pass dichroic filter coated on each side with two different WLS. The external shifter converts the 127 nm LAr scintillation photons into a photon which the wavelength is below the filter's cutoff, and so it is assumed to be transparent, while the inner one shifts the light to a wavelength above the cutoff turning the filter is reflective. The net result is that the photon get trapped inside the highly reflective box and it will end by being detected by the active photosensors installed on its internal surface.(10)

To become a X-ARAPUCA the inner shifter is substituted by a an acrylic slab which has the WLS compound embedded. The active photo-sensors are optically coupled to one or more sides of this slab, as shown in figure 8. And so there are two main mechanisms through which a photon can be detected by the X-ARAPUCA:

1. Standard ARAPUCA mechanism. The photon, after entering the X-ARAPUCA box, is converted by the WLS of the inner slab, but is not captured by total internal reflection. In this case the photon bounces a few times on the inner surfaces of the box until when it is or detected or absorbed (figure 8,left);
2. Total internal reflection. The photon, converted by the filter and the slab, gets trapped by total internal reflection. It will be guided towards one end of the slab where it will be eventually detected. This represents the first improvement with

respect to a conventional ARAPUCA (figure 8,center), which contributes to reduce the effective number of reflections on the internal surfaces. The sides of the slab where there are not active photo-sensors will be coated with a reflective layer allowing to keep the photon trapped by total internal reflection.

Figure 8 – Left: Standard ARAPUCA mechanism. The photon enters the box, it is converted by the WLS slab and is captured inside the ARAPUCA. Center: Total internal reflection. A converted photon enters the box and it is converted by the WLS in the slab and trapped by total internal reflection. Right: High angle photons. A photon with high incidence angle inside the box, is trapped in the liquid argon gap between the filter and the acrylic slab. Notice that in this last case the guided photons are not shifted by the slab (10) .



Source: Machado *et al.* (2018, p.3). (10)

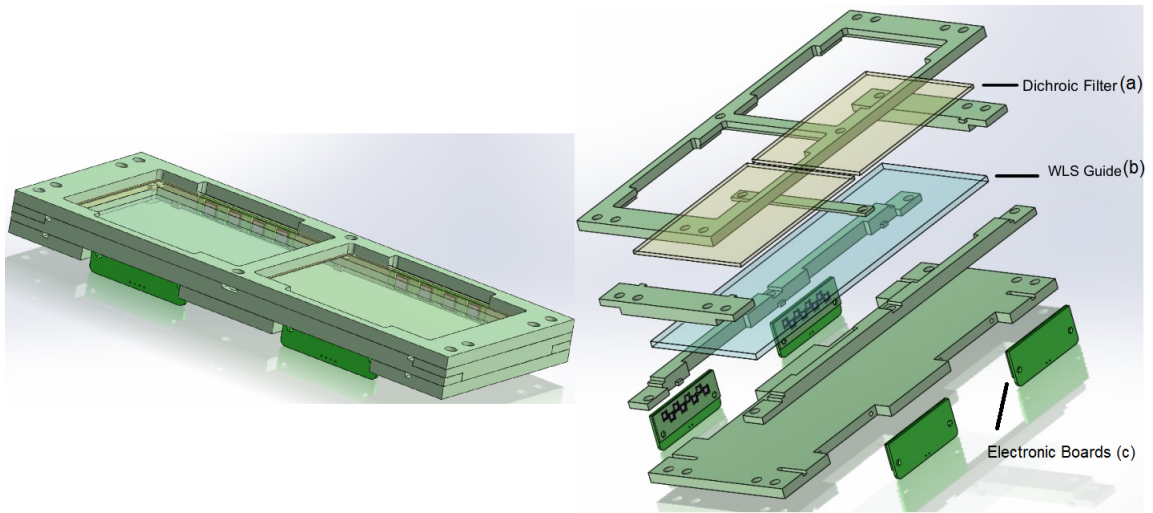
### 5.1.1 Arapucas Structure

Within the X-Arapuca concept it is possible to fit the structure and dimensions to fit in several geometric and needs. For SBND the modules were designed in a way to fit replacing the original photomultiplier inside the PD-Boxes with minimal changes on it. For being able to detect both visible and UV light each "slot" where it used to have a photomultiplier were replaced by an UV X-Arapuca and a visible (coated) X-Arapuca positioned side by side using an adapter plate.

The X-Arapuca bodies are formed by G10 plates made by water-jet cut and hold together by a set (6 pcs) of screws and nuts. This structure is able to make two windows with dichroic filters and also hold in place the electronics boards and the wavelength shift guide (WLS) as seen in figure 9. Other parts were added to hold the X-Arapucas in the correct place.



Figure 9 – Left: A Frame of one SBND X-ARAPUCA module as it is assembled Right: An exploded view of the the module showing its internal components (a) dichroic Filter, (b) WLS Guide, (c) Electronic boards.



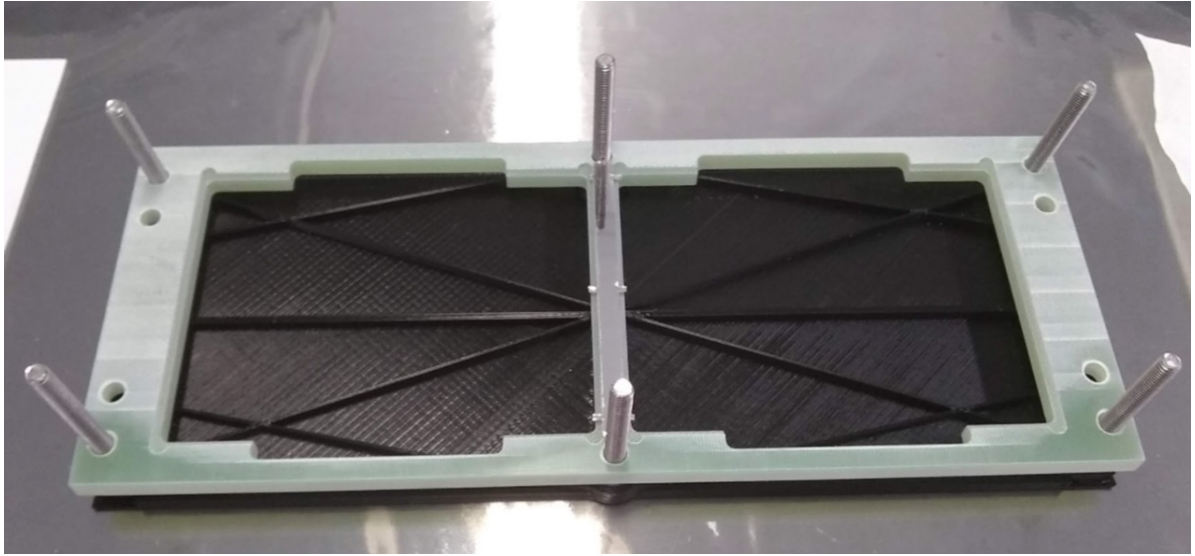
Source: Machado *et al.* (2018, p.8). (10)

The main parts in the X-Arapuca set are:

- G10 Frame

As it is seen in figure 10 and also in figure 9 the outer structure of the X-ARAPUCA is made of G10/FR-4 that is a composite material that consists of glass fabric, electrical grade epoxy resin. The material is extremely strong and stiff, has a low coefficient of thermal expansion, and outstanding electrical properties. G10/FR-4 is widely used as an insulator for electrical and electronic applications and also showed to have good cryogenics properties.(44) This structure has the roles of holding all the components in correct place and also have the mounting holes for assembling the X-ARAPUCA in the working place.

Figure 10 – A view of the internal part of a X-ARAPUCA front G10 frame with the holding screws and the 3D printed covers



Source: Author (2023).

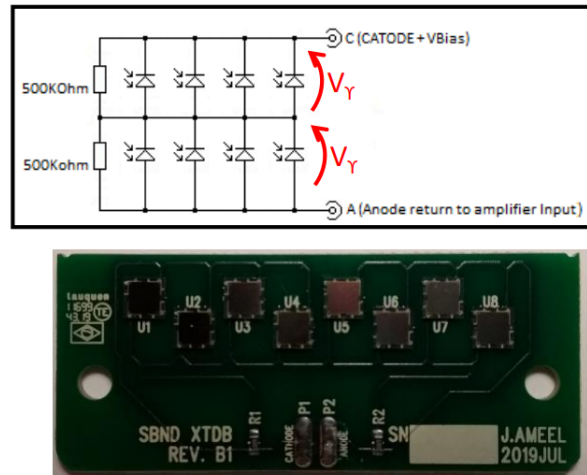
- Electronics boards and wires

The electronics boards holds the SiPm's and the electrical components in place and also make it possible the attachment of the wires to read its signals. They are attached in the sides of the X-ARAPUCAS as seen in figure 9. They have two models with differences in the SiPm sizes and the wiring diagram.

- The X-TDB Electronics boards and wires for Daphne readouts:

The X-TDB boards have the role of being the interface between the SiPm sensors and the wiring for the Daphne interface. This model of electronics holds eight 3x3 sensors installed in sets of four in parallel in series of another set of four, as seen in figure 11. This interface is wired with two wires one cathode (+Vbias) and one anode (that goes to the interface input).

Figure 11 – X-TDB Electronics board with electronics scheme

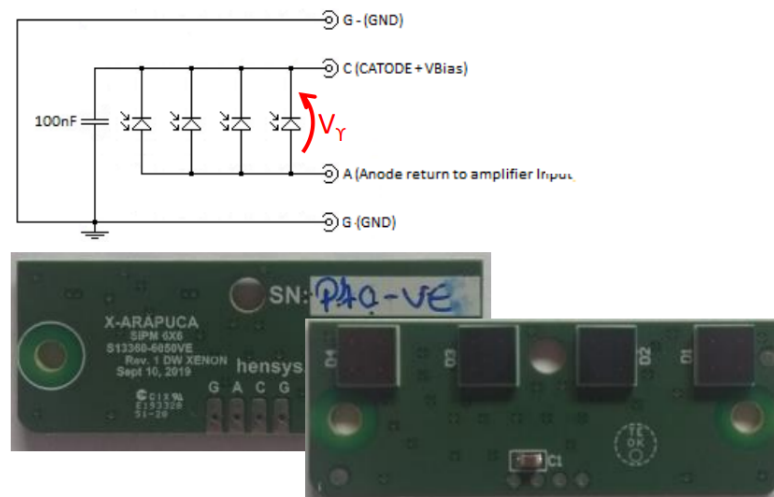


Source: Author (2023).

- The X-ASB Electronics boards and wires for APSAIA readout:

The X-ASB boards have the role of being the interface between the SiPm sensors and the wiring for the APSAIA interface. This model of electronics holds four 6x6 sensors installed in sets of four in parallel, as seen in figure 12. This interface is wired with four wires one cathode (+Vbias), one anode (that goes to the interface input) and two ground that loops around the board for shielding it.

Figure 12 – X-ASB Electronics board with electronics scheme



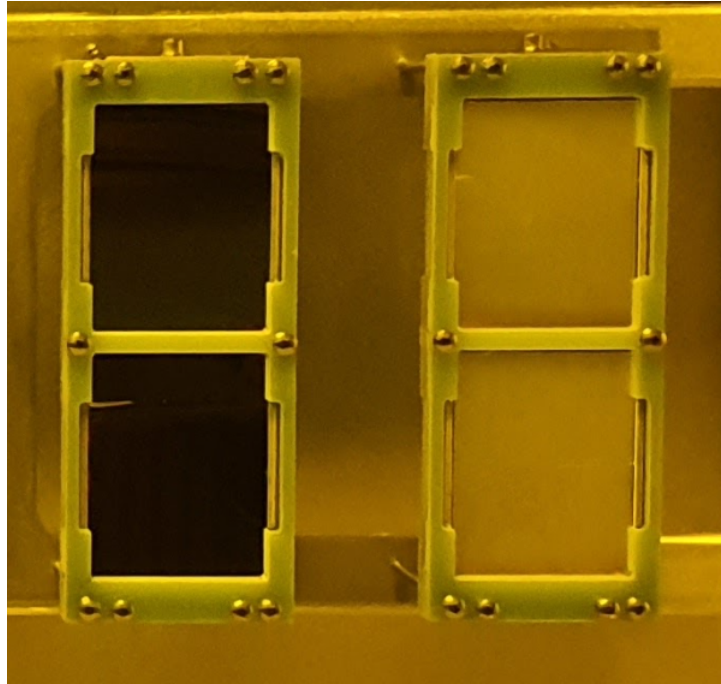
Source: Author (2023).

- dichroic filter

The optical aperture for the X-Arapucas are made using dichroic filters. This elements are responsible for letting the light go inside by a high transparent window and be

very reflective for the shifted light, trapping it inside the device. Those elements are installed in the very front of the detector and have two kinds one not coated for visible light, as seen in figure 13 (left) , and one coated with a wavelength shifter for UV light, as seen in figure 13 (right).

Figure 13 – A view of two X-Arapucas side by side where it possible to see the one with not coated dichroic filters (left) and the one with coated dichroic filters (right)

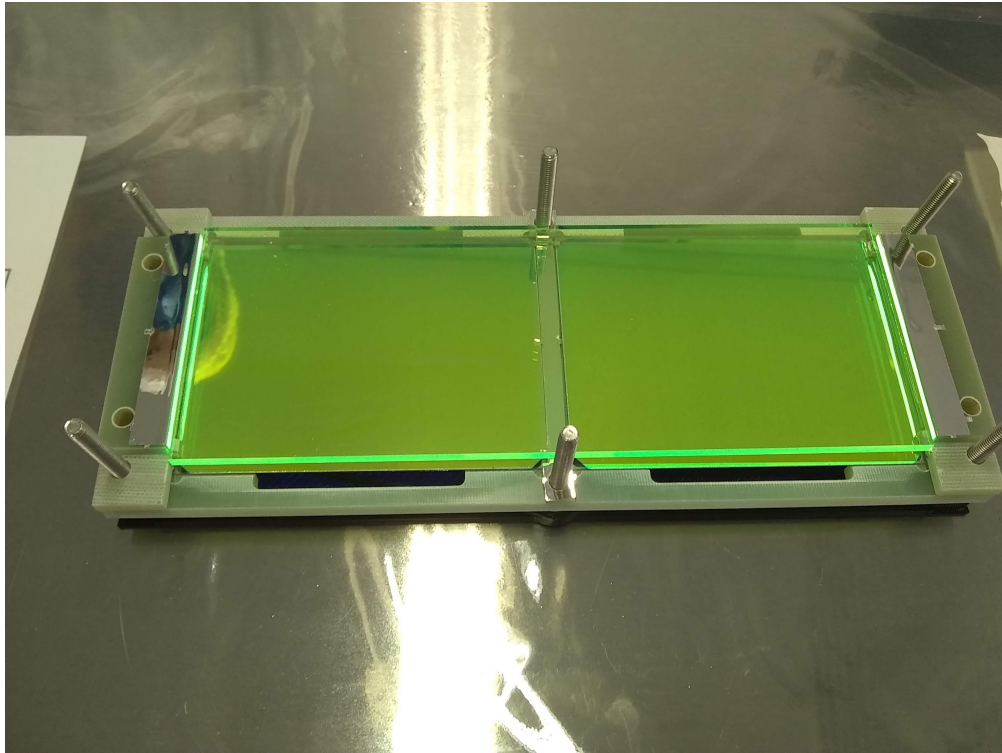


Source: Author (2023).

- WLS

The WLS plates are a element that is installed along the right middle of the X-Arapuca. This element have two functions one is two shift the wavelength of the light inside so it get trapped by the dichroic filter the other one is to guide the light to the front surface of the SiPm sensors, the place of installation can be see in the half open device in figure 14.

Figure 14 – A view of the WLS plate installed inside a half open X-Arapucas



Source: Author (2023).

- Mounting structure

The mounting structure is a set of elements that will allow a pair of X-Arapucas been installed in the PD-Box in the same slot replacing a photomultiplier that used to be in the box.

- Standoffs and Screws

The standoffs are elements that have been custom made for mounting the X-Arapucas in the appropriated height so it will be the most possible height that will not shadow the photomultiplier in the sides close by. The screws are standard fixing elements used to hold everything in place, all those elements can be seen in the figure 15.

Figure 15 – A set of 8x Standoffs and all the M5 screws washers and spacers for mounting one set wit a pair of X-Arapucas.

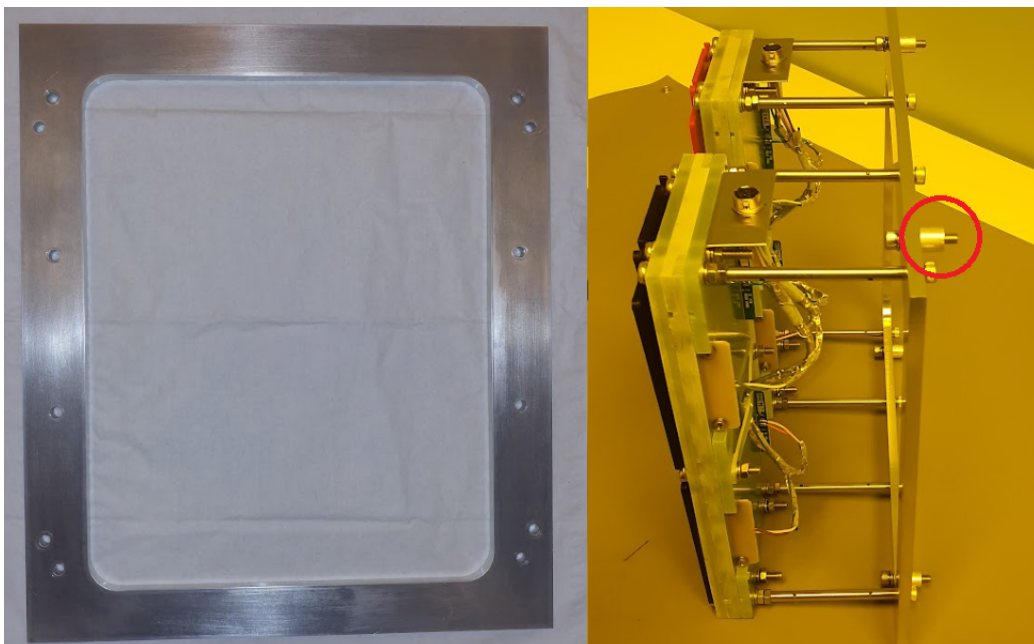


Source: Author (2023).

- Adapter plate and spacers.

The adapter plates are a solution to hold two X-Arapucas in the slot in the PD-Box where it was designed to install a photomultiplier. It consists of an aluminum plate with the holes for all the needed fixing elements as seen in the figure 16 (left). Also there are aluminum spacers that allow the adapter plate to be mounted in the PD-Box as seen in figure 16 (right).

Figure 16 – The Adapter plate mount for assembling the X-Arapucas (left) and a set of Two X-Arapucas mounted on a Adapter plate (right) where the one of the aluminum spacers are highlighted.



Source: Author (2023).

### 5.1.2 Clean tent and Working Bench

The X-Arapucas device are a very light sensitivity element, also they require a very clean handling to keep the desired efficiency. For that a setup was arranged a clean tent in the assembly local (Fermilab Batavia Site, D-Zero building in the annex room). This tent was made of an Unistrut frame and Herculite tarp walls. Inside it was placed working benches for the correctly handling and for accommodate the suitable assembly procedure. It was also set up cabinets for accommodating the "ready to go" device and all the parts and tools for the assembly.

### 5.1.3 Assembly Procedure

The entire procedure must be performed in a controlled environment, under yellow lights. The operator must use the PPE suitable for controlled environment.

The device was sent to Fermilab previously assembled so the assembly procedure on it was resumed to install the electronics in each device in a procedure as follow the steps.

- Clean the X-TDBs cables and L-bracket with ESD-safe cleaning wipe. Be careful to not unwrap the shield protection.
- Clean the flux solder using toothpick with cotton tip moistened with ethyl alcohol. Clean the SiPM's window with anti-static foam swab moistened with a 20% solution of isopropyl alcohol diluted in deionized water. Be careful to not damage the SiPM's surface.
- Open the package with a retractable utility knife and remove the module.
- Using a reversible ratchet wrench (8 mm) and a phillips screwdriver N.2, release the necessary screws for removing the covers (see figure 17, installing the connector bracket and holding the tension relief clip).

Figure 17 – X-ARAPUCA cover screws

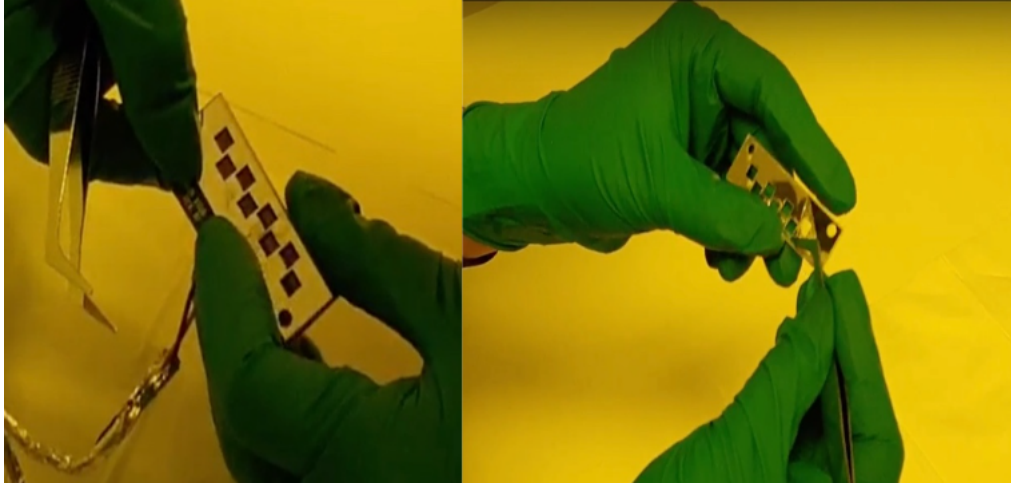


Source: Author (2023).

- Position the bracket (on the back side of the module) on screws 7 and 8. Place the flat, split lock washers and the nuts, re tighten the screws 7 and 8 (by hand).
- With tweezers, remove the protective film of reflective adhesive from SiPM's mask, be careful to not scratch the surface as seen in figure 18 right.



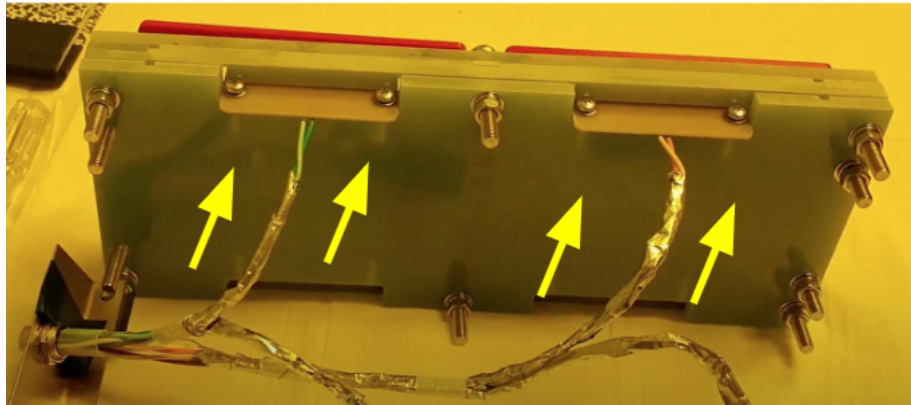
Figure 18 – Boards protective film of reflective adhesive installation and handling



Source: Author (2023).

- Position the SiPM's mask on the SiPM's electronic board (seen in figure 18 left) and install the SiPM's board in the electronic slot on the sides of the X-Arapuca (showed in figure 19), the SiPM's board with the mask positioned must be faced inside the module. Fix it using conical washers and the M3x0.5 screws. Repeat for the 4 boards.

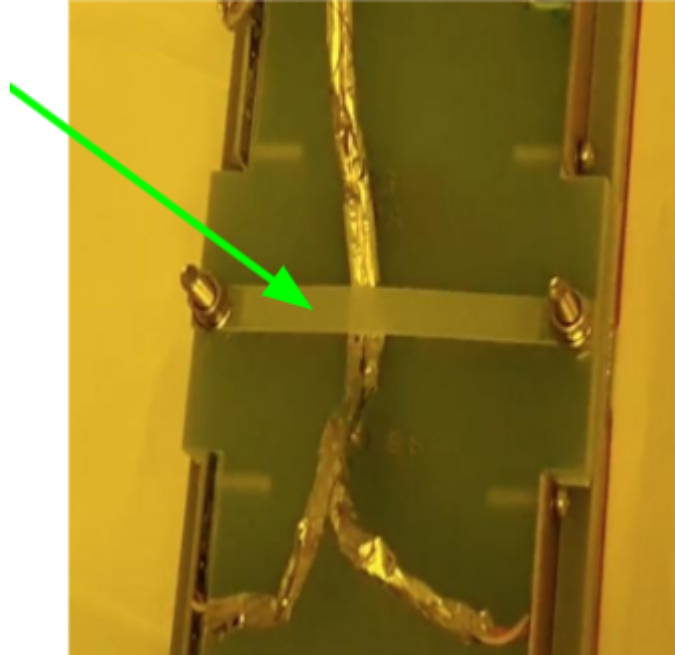
Figure 19 – Electronics boards insertion



Source: Author (2023).

- Turn the module so that it is back facing up, place the cable strain relief bar (smooth side up) holding the cables as seen in figure 20. Make sure the cables are not stretched.

Figure 20 – Stress relief bar instalation



Source: Author (2023).

- Using a torque screwdriver (M5 Phillips bit) and a wrench 8mm, tighten M5 all the screws to final torque of 4.0 Nm.
- Tighten all screws of SiPM's boards with final torque of 1.2 Nm using a torque screwdriver (M3 Phillips bit).
- Storage the X-ARAPUCA inside the proper package with two silica gel bags attached.

#### 5.1.4 Quality control

For the assembly the Quality control is necessary to be sure all the assembled devices are correctly assembled, all the components are proper working and it is ready to be installed.

The first inspection is a visual check on the electronics boards solder. Looking for both excess or fault amount of solder, the correct place of the wires and the rigidity of the cable holding. The same is made in the connectors end to check the assembly.

A check of the electrical resistance and the DC tension in the board is made in the electronics before the assemble and after the assembly using a test interface board that connect in the device after assembled.

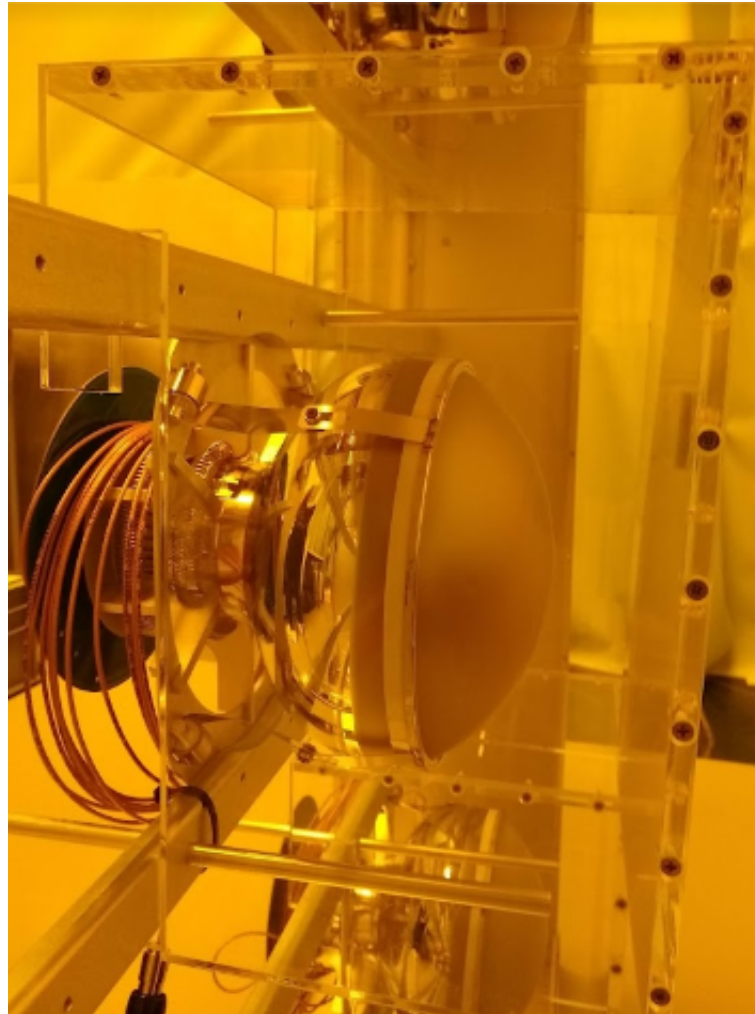
## 5.2 PHOTON DETECTION BOXES

The SBND photon detection system is a modular structure made of 24 PDS boxes. Those boxes are an element that holds five 8" photomultipliers and eight X-Arapucas. They are made in a way that makes it possible to assemble them in the sides of the detector with those elements already installed on it which make easier working on proper environment and transporting to the final local installation. The boxes also have covers to keep the elements safe during the storage and the full detector transport.

### 5.2.1 PMT's Assembly in PD-Box

The 8" Hamamatsu photomultipliers were sent already installed in the PD-Boxes. The boxes also worked as a mechanical and lightproof storage for it while they were waiting for the installation. Because they were previously assembled, covers were designed to protect the PMT's during all the other works going on inside the boxes (as show in [figure 21](#)).

Figure 21 – PMT tube with cover installed



Source: Author (2023).

### 5.2.2 Arapucas Assembly in PD-Box

The X-Arapucas are installed in the PD-Box replacing a slot where it used to be a Photomultiplier, for that an adapter plate is used (figure 16) that will hold two X-Arapucas inside the box. Each box use 4 plates to mount the 8 X-Arapucas. The procedure to install that devices on it will be described as following.

### 5.2.3 Assembly Procedure

Owing to the inherent light sensitivity of the system, it is imperative that the entire assembly procedure be meticulously conducted within a controlled environment, illuminated exclusively by yellow lights. Operators undertaking the assembly are mandated to don Personal Protective Equipment (PPE) specifically designed for use in such controlled

environments, ensuring both the integrity of the delicate components and the safeguarding of the operator.

The mechanical assembly procedure follows a systematic sequence:

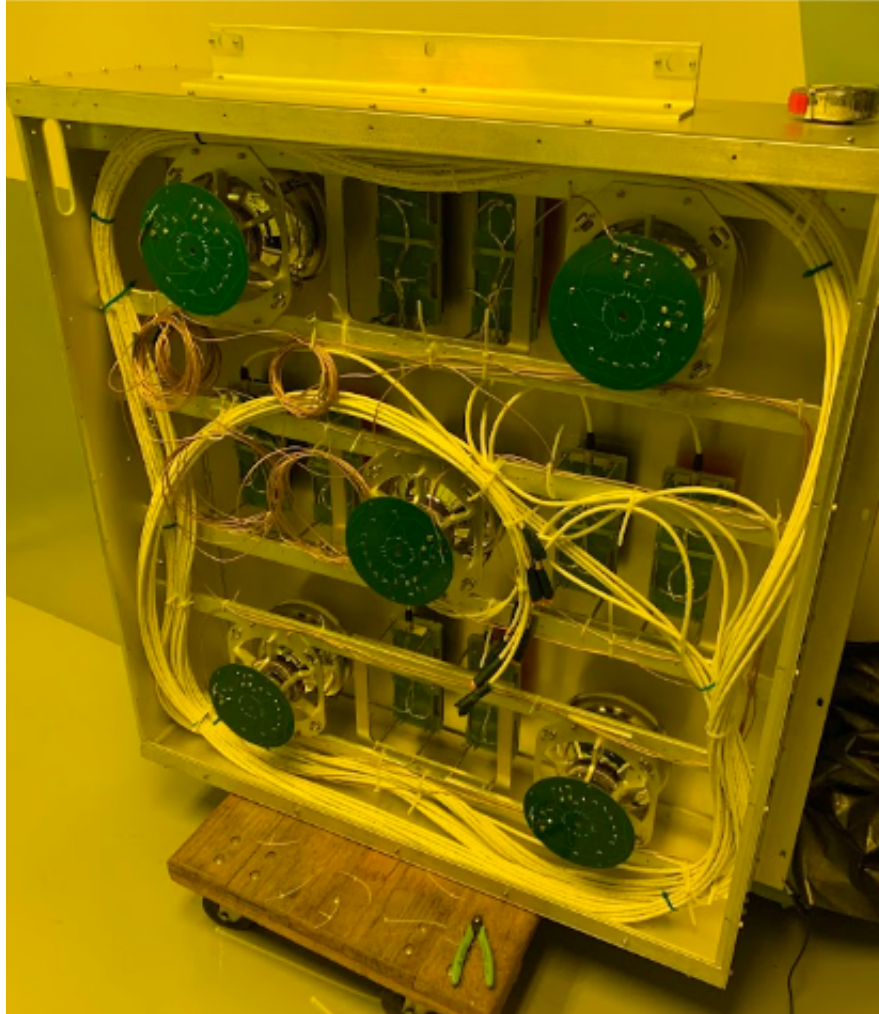
- X-Arapuca pairs preparation
  - Place the X-ARAPUCA face down and L-bracket to front. The VIS (red cover) on the left side and the VUV (black cover) on the right side for the sets to assembled in the top position. For the ones assembled in the sides and bottom, place the X-ARAPUCA VUV (black cover) on the left side and the VIS (red cover) on the right side.
  - Install the standoffs on the four corner screws of each module.
  - With the modules facing down, align the holes in the adapting plate to the standoffs.
  - Place eight screws M5x16 mm with split lock washers to fix the adapting plates on the standoffs threads. Using a torque screwdriver (Hex bit 4 mm) tighten the eight socket head screws with final torque of 4.0 Nm.
- PDS-Box Preparation
  - Remove the front and back lids of PDS box.
  - Protect all the PMTs with the acrylic covers;
- X-Arapucas sets installation
  - Place four screws M5x25 mm with split lock washers and on the back side of adapting plate, place one spacer on each screw to fix the adapting plate on PDS box bars using a L-key 4 mm.
  - Install the set in it slot. For the top adapter plate must be with brackets and Hirose connectors facing to bottom. For the sides and bottom adapter plates the brackets and Hirose connectors may be facing to top.
- Remove the PMTs acrylic protections and put back the front and back lids of PD box.

#### 5.2.4 Wiring and Pre Routing

The devices inside the boxes need to be wired, the X-Arapucas use cat6 cables connected by the hirose connector and the PMT's use a high voltage coaxial cable soldered direct to the control board on it. Those cables need to be attached to the devices and be safely stored installed inside the boxes before they being assembled in the detector. So all

the cables are installed and pre routed inside the box in a way it is attached to the walls and loop around the box to be safe during the transportation and installation as show in figure 22. Also they need to be easily removable thought the hole in the side to be routed to the feedthrough position in the cryostate.

Figure 22 – PDS box with the wires routed the position inside the box



Source: Author (2023).

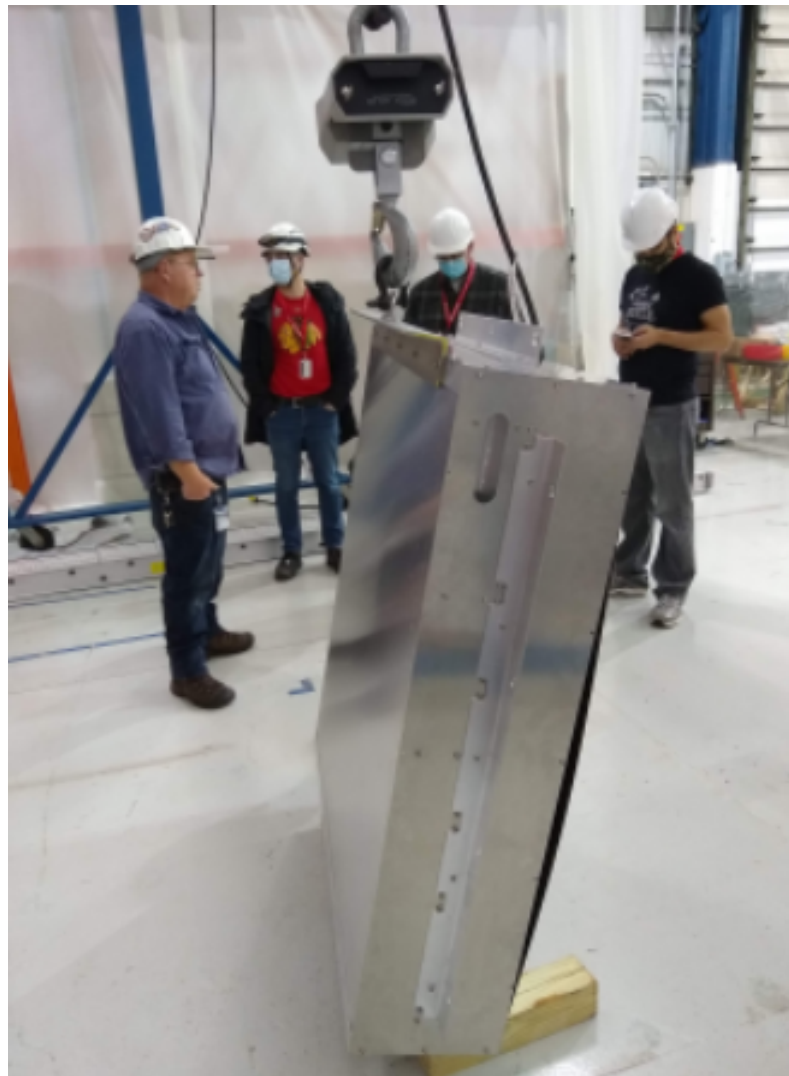
### 5.2.5 Storage and Protection

After all the inside work is done all the boxes have the covers placed to protect the devices and cables in it, this covers provide both mechanical and light protection when the boxes are stored or being transported around. The boxes ready to go to the assembly position are stored in a room free from UV and blue light and also covered with a tarp that provide extra light protection and prevent from dust on the boxes.

### 5.2.6 PD-Box Lifting Bar

The final place where the boxes need to be installed is in the detector wall, that slots are above the floor level and it makes necessary the boxes to be hung but the original design didn't had a hanging point and the mounting holes could not be used to hang as any hook or attachment device would block the the surface that should touch the detector wall. A lifting bar was proposed and tested to fulfill that function, this bar could be assembled in the threaded holes that was used to hold the covers in the back of the boxes. This device need to be approved by the fermilab safety standards and go through a load test (seen in figure 23) before put in use.

Figure 23 – Mock PDS box attached to the lifting bar during the load test



Source: Author (2023).

### 5.2.7 Quality Control

To ensure the proper functionality of all components within each box, rigorous testing procedures were executed upon the completion of assembly, confirming the readiness for operational deployment. The conducted examinations encompassed the following tests:

- Electrical connection X-Arapucas

Upon the installation of all X-Arapucas and associated cables, a comprehensive evaluation is undertaken utilizing a specialized test interface board. This examination involves the precise measurement of electrical resistance and dark tension. Significantly, this test assumes paramount importance as it occurs at the terminal stage of the connector, thereby enabling the detection of potential issues spanning from the device to the connector, ensuring thorough diagnostic coverage.

- PMT cables Solder

The photomultipliers employed within the boxes incorporate an electronic board in their rear, as is customary, hosting critical components essential for the proper functioning of the apparatus. All wiring cables are meticulously affixed to this board. To ensure the optimal performance of the photomultiplier tubes (PMTs), comprehensive testing is conducted on the soldered joints of both components and cables. This testing includes examinations for continuity and the absence of shorts, with any necessary reworking undertaken promptly.

- Light pulse test X-Arapucas

A specialized testing plate, replacing the front PD-Box cover, has been devised. Equipped with Light Emitting Diodes (LEDs), this setup creates a controlled darkened internal environment when the box is closed. Pulsating LEDs mimic light signals, replicating realistic operating conditions for the X-Arapucas. The X-Arapucas are powered using suitable Data Acquisition (DAQ) systems (APSAIA or Daphne), with pulsating LEDs simulating authentic light signals. This setup enables the measurement and analysis of the devices responses under controlled conditions. This testing protocol encompasses the full spectrum of X-Arapucas functionalities, from sensors to wiring and cables and the DAQ. The simulation mirrors real-world scenarios, offering a comprehensive assessment of the devices in environments where they are intended to be deployed.

- Dark test in PMT

Similar to the X-Arapuca the test of the PMTs is made with the box full covered. In this setup, stopping muons serve as the light source. When the box is closed, the internal environment is controlled and darkened, allowing for precise measurement



and analysis. PMTs are powered using a high voltage power supply and the readout is made by an oscilloscope, stopping muons act as the light source, enabling the measurement and analysis of the PMTs' responses under controlled conditions. By subjecting PMTs to this test, the goal is to ensure individual reliability and collective resilience. This approach identifies and addresses potential issues, contributing to the overall enhancement of PMTs' performance and durability in the operational settings.

- Cables attachments and connectors

The conclusive assessment involves a meticulous examination of cable attachments, primarily conducted through visual inspection and careful pulling. This procedure is undertaken to ascertain the robustness of connections and to verify the presence of necessary strain relief attachment points. Additionally, succinct electrical continuity checks are performed to ensure the adherence of electrical connections to prescribed standards. This verification focuses notably on the grounding wires, ensuring their appropriate connection where required and their intentional non-connection where deemed inappropriate.

### 5.3 THE INSTALLATION OVERVIEW

Once completing the preparation of the PDS-Boxes, the subsequent step involves integrating them into the detector walls. This integration includes securing the boxes in place and carefully routing cables to the designated flange position. As the detector readies itself for relocation to its final position, meticulous attention is given to ensuring robust attachment and security. Covers and temporary holders are strategically employed to enhance light impermeability and fortify shock resistance for the light sensors.

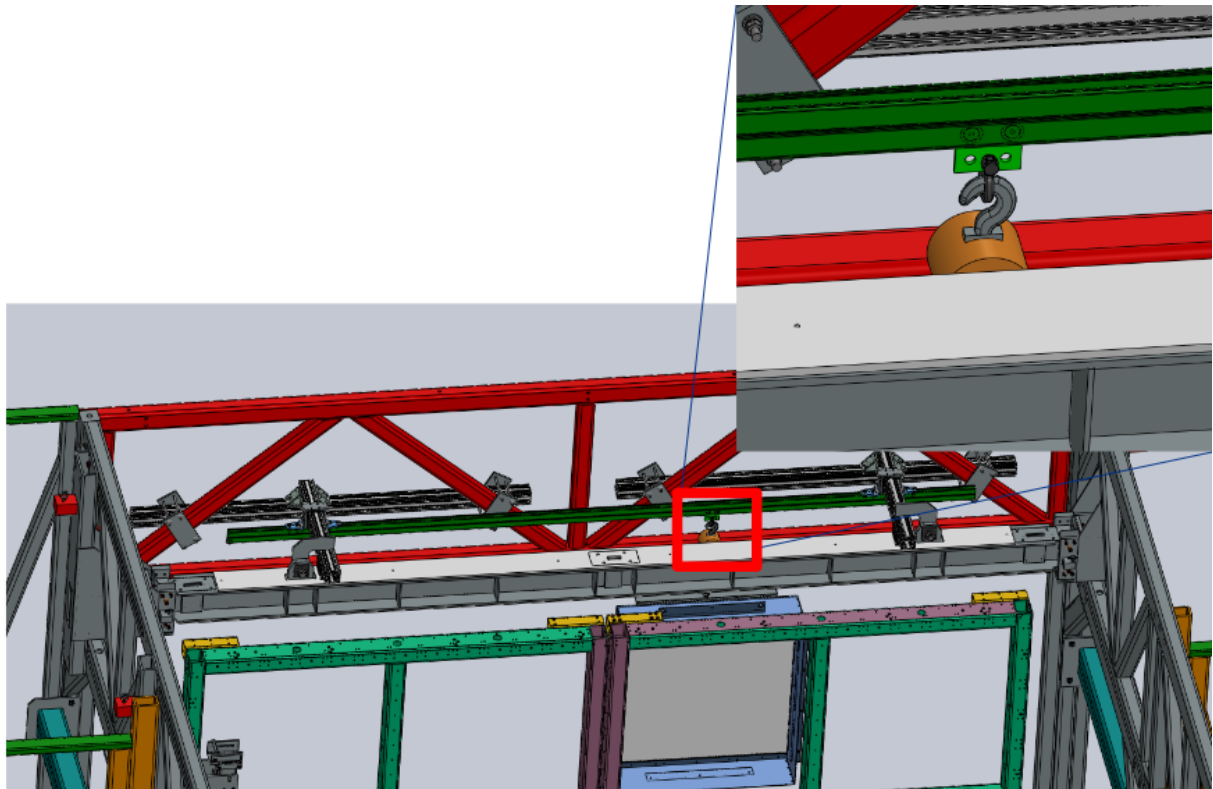
Throughout this intricate assembly process, delicately suspending and maneuvering the boxes to their ultimate position under a clean lightproof tent that envelops the entire detector in the assembly bay is imperative. This precautionary measure is implemented to safeguard against contaminants such as dust moisture or vapors and maintain optimal conditions for the assembly process establishing an area free from UV and blue light also keeping the operators far from tripping hazards and other people not aware about the work being conducted.

#### 5.3.1 Hanging structure

A structure for lifting the boxes is not included in the ATF also the building crane is too big to go inside of the ATF roof and the sides are too far from the APA. To overcome this a side structure was designed to lift the boxes. This structure is attached to the

ATF and have a movable attachment to allow the chain crane to be moved to the many necessary positions. The lifting structure and the hook attachment can be visualized in the model shown in the figure 24.

Figure 24 – Model of the lifting structure mounted in the ATF with an expanded view of the hook attachment



Source: Author (2023).

### 5.3.2 Problems and Concerns

The first challenge for the assembly was to move the boxes from the clean assembly room to the detector position while keeping it clean and light safe. Its were made with the use of plastic covers over the aluminum closing covers on the boxes and the movement made with a proper cart by hand one by one by hand by two operator while a third one took care of the clean path.

Also as the boxes have sharp edges the handling were made with sometimes heavy duty gloves sometimes with clean gloves for the delicate parts close to the sensors. For this work the tasks were divided in a team where which member had a unique set of tasks suitable with his owned tools and PPE set. A big concern during the installation was that the boxes should be hung in a limited space and handled, which means pushed inside the detector by hand, very close to the APA wires planes. A lot of studies about the go in angle and the depth of the mounting blades were made to be sure that a touch on the

wires would be mechanically impossible.

### 5.3.3 The covers and protections

Two main groups of covers were used to keep all work clean and lightproof

- Covers attached or over the boxes This group of covers include the aluminum covers in the front and in the boxes in all the boxes, that covers have the role of keeping the box mechanically robust for in case of a crash or some hit in the box it have a minimum chance of damaging the sensors inside. Besides these covers this protection system also have aluminum rods installed inside the boxes around the PMTs to prevent the covers itself to touch the surface of the PMTs. Those covers are attached by a sliding slot on the boxes and secured with screws on the side. They must be used while transporting the boxes but must be removed for the final installation.
- ATF covers and walls. Around the ATF and detector walls were made plastics covers to keep the inside part clean ans also lightproof. All that walls were checked and replaced when needed before the PDS installation to make sure no excessive light would be inside when the sensors are exposed once the front cover can not be in place when the box is attached to the APA. This covers will be very reinforced and a second opaque cover will be placed for the detector move.

### 5.3.4 The PDS installation team and functions

In the assembly team there was some functions, each functions had a set of roles, tools and parts to check, except for the chain operator that required an special safety training all other functions where shown ans explained to all team members who could perform any of the function and decided based in which one felt more comfortable. The key functions are:

- Chain Operator This operator is supposed to have passed the training for portable crane operator and be lift trained. The roles of this functions is to operate the hook chain and be in charge of oversee all the hanging operation safety. Also this operator will position the hook in the lifting structure, inspect the lifting bar and the eye bolt, attach the hook and operate the scissor lift when needed. As this operator uses a pair of heavy duty gloves and they are not appropriate clean it will avoid to touch the box and the APA. The tool set for this operator is a 3mm Allen key, a 10mm wrench for inspecting the lift bar installation, heavy duty gloves and some Small ropes or tape to secure the chain when needed.

- **Chain Assistant** This operator have the main role to watch and handle the chain when it is moving close to the APA also control the area around the lifting work, signalize for people don't enter the area and inform the chain operator when it is safe to move. The tool set is a long rope to hold the chain from the floor, sets of ropes to move the chain to the sides and small ropes or tape to secure the chain.
- **Box Handler** The box handlers are two operators, they must be lift trained, they will make the box attachment itself. The box handlers are in charge to check the box for any moving element that could be in the way of assembling or damage the devices in the box. They need to know very well the assembly position of each box and point to the chain operator. They will handle the box when it is above one and half meter for the most top boxes and handle it from the floor for the bottom boxes. They will give instructions to the chain operator during the whole procedure and wear clean laboratory gloves to be able to touch the box and the APA. When the boxes are in position they will push it and install all the screws an components. Also they are in charge of the final checkups in the installation. The tool set for the Box Handlers are: Long and short "T" shaped 3mm Allen keys 10mm wrench. And they need to make sure they have the accessories (and also spares): two long (40mm) M5 Allen screws, ten sets of small (16mm) Allen M5 screws with flat and lock washers, four sets of medium (20mm) M5 Allen screws with Large washer and lock washer, bottom box bracket with screws and nuts, back cover for the box with at least four screws.

- **Floor Box Handlers**

The Floor Box Handlers are also two operators, they will be in charge of all the box handling in the floor that starts in the assembly room with the checkups and the covering, the move to the ATF tent and the uncover and covers removal. Remove the front covers of the X-Arapucas and re tight the screws Also the positioning for the lift bar install and the move from the cart to the ATF floor. When the box is being lifted they will guide it from floor to the firsts one and half meter. Also for the bottom boxes the floor handlers can act as Box Handlers and install the boxes. The tool set for the Floor Box Handlers are: 3mm Allen keys, sets of clean heavy duty gloves and laboratory gloves, cutting pliers and spare zip ties to secure cables, phillips screwdriver N.2, torque screwdriver (M3 Phillips bit), 10mm wrench and cleaning wipes.

### 5.3.5 Work Procedure

The installation procedure starts when the box is assembled and ready to go in the clean room. The first step is to put it on the cart by holding it in two people tilting it to

one side while it stay touching the ground, position the cart in about the middle of the box and tilt it back to horizontal on top of the cart. This procedure needs to be made in a way that the box don't get shocks or hit anything in its way. Once it is in the cart it is needed to wrap it with an opaque tarp that will protect it from dust and light. The tarp can be secured by tying up with ropes or even with duct tapes.

Once covered the box need to be moved to the ATF location. It is made by pushing it carefully by two operator to make sure it will not get off the cart while a third one check all the way for obstacles and opens doors and the aperture in the tent.

When the box is inside the tent and the door is closed the tarp can be removed. It need to be checked if there are no dust o damages in the box. When all check is okay the front and back covers are removed by hand taking care with the sharp edges, also the all aluminum rods need to be removed paying attention if the screws come out with then and removing if not.

Next step is to remove the front X-Arapucas covers by releasing (not removing) the two bottom screws on the modules, removing the covers by pushing it up with care to don't touch the glass surfaces. when removed tie the screws back using the torque screw driver. During this procedure also check if all PMT's connectors are well attached to the boxes and all grounding flats of the X-Arapucas are attached connected.

Now it is need to install the lifting bar (note once handling the lifting accessories and tools the inside the boxes devices can't be handled without changing gloves). It is made by two operators while one holds the bar in position the second attach the screws in the top thread holes on the back of the box. Make sure all the screws use flat washers in the screw head side. when all screws are in position the flat washers and nuts may be installed in the internal part. Lot of care because they will be mounted very close to the detectors. When all the screws are done and checked the eye bolt is installed in the top lift bar with the nut in its bottom. The eye bolt may be already installed in the bar if this happens it need to be checked by releasing and attaching again the nut.

The fully fitted and with lifting bar box need to be placed in front of the column to the designated position. It is made placing it as near as possible with the cart and pacing it by hand by two operators in the ATF floor. It is not hung directly from the cart to prevent it from swing and hit the APA. With the box sitting in the ATF floor the scissor lift is positioned parallel to the box and APA with middle of the scissor lift about aligned to the middle of the box. The chain hoist is positioned in the hanging structure with the hook aligned to the middle of the disordered APA slot. The chain operator maneuvers it until the hook reaches the the eye bolt in the box while the chain assistant takes care for the chain doesn't touch the APA. And finally attach the hook in the eye bolt.

The installation will be made column by column in any order and row by row

always starting from the top row and the following procedure depends on which row the box is installed as following:

- Top Row:

For the top row it will be needed in the scissor lift the chain operator and two box handlers and in the floor the chain assistant and two box handlers with all the tools and accessories that will be listed below. In the first stage while the box is less than one and half meter from the ATF floor the chain operator will start lifting the box by pulling the chain and the floor box handlers will guide it from the floor paying attention if the lifting is smooth and is not touching neither the APA or the scissor lift. Passing the one and a half meter the box will be guided by the box handlers in the lift. When the box is too high for the handlers the scissor lift needs to be operated by the chain operator who will secure the chain in the lift edges and slowly move up. The moving up can be divided in small steps going a bit up and operating the chain to move the box in a way that the handlers feel comfortable by holding it and repeating until the box arrive in the desired position.

- Middle row:

For the middle row it will be also needed in the scissor lift the chain operator and two box handlers and in the floor the chain assistant and two box handlers with all the tools and accessories that will be listed below. Similar to the top row in the first stage while the box is less than one and half meter from the ATF floor the chain operator will start lifting the box by pulling the chain and the floor box handlers will guide it from the floor paying attention if the lifting is smooth and is not touching neither the APA or the scissor lift. Passing the one and a half meter the box will be guided by the box handlers in the lift. At this point it may be necessary just a small move up with the scissor lift or not the box handlers will decide it.

- Bottom row:

For the bottom row it will not be needed in the scissor lift, the chain operator the two box handlers and in the chain assistant will be in the floor with all the tools and accessories that will be listed below. Now the chain operator will start lifting the box by pulling the chain and the box handlers will guide it from the floor paying attention if the lifting is smooth and is not touching the APA. It will be necessary just a few moves in the chain to get in position.

Once the box reach the desired slot it need to be pushed inside the slot by the two handlers, it can make easier if the box is lifted a bit higher and the chain operator slowly release it while pushed, when pushed inside one of the handlers will hold the box in place while the second use a pair of longer screws to secure the position, it is preferred to use

the most upper assembly hole but if it is not easy the second can be used, the long screws do not need to be pushed all the way inside as they have the role of just guiding the box in place. Now by a visual check the assembly holes must be aligned by small moves on the chain, when it looks good the final screws are placed by hand with no final torque letting the longer one to be replaced as last one. when the side are done it must be installed the three top ones, paying attention for its bigger washers. with all screws in place apply the final torque in all of them. When done, the boxes handlers attach the bottom holder bar on the box and attach the holding screws on it. The chain operator release the tension on the chain, now the box is attached to the APA the lift bar is removed, taking a lot of care with the inside nuts, the lift bar can both be detached from the chain and removed by hand or kept on the chain and the operator down and secure it before detach. When the lift bar is removed the box handlers install the back cover on the box starting from the top screws. It is not needed to install all the ten screws for the cover as it will be removed for the cabling, four screws two on top and two on bottom are enough. And the box is installed.

### **5.3.6 The pos installation checkups**

After the installation is done there are some checkups to be made to ensure everything went okay, those checkups are

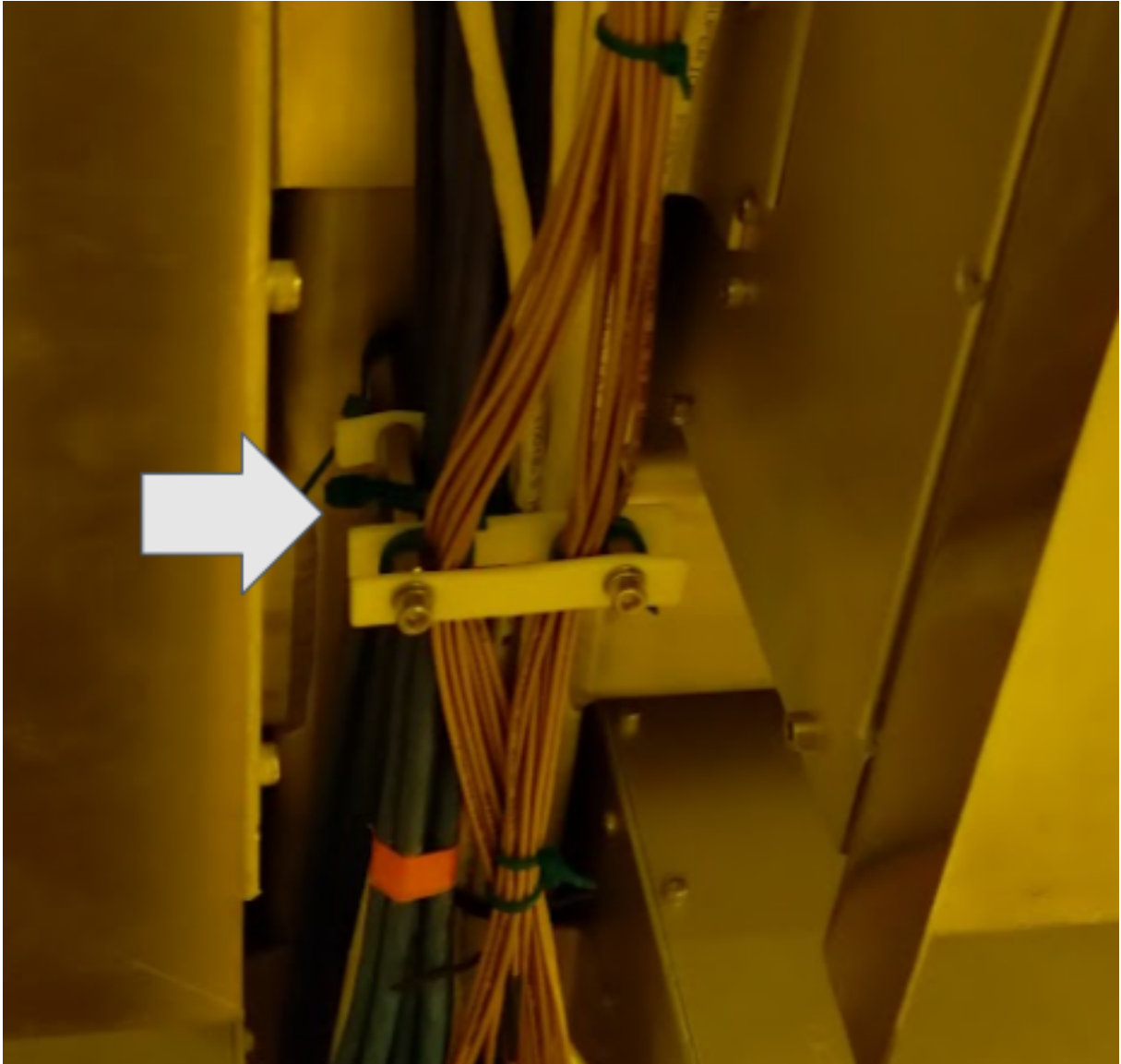
- Check all the boxes for all screws in place, check is all the bottom holders are correctly installed. Check if all flat washers are in place and not bent or deformed. Check if all screws hav a lock washer.
- Check if the threaded holes used for lifting are not damaged or the top bar is bent.
- Check if all the connector keep attached and the cables are safe inside the box.
- Check if all the covers have at least four screws two on top and two on bottom.
- Check if all the boxes have the edge protector in the cable window and at least two cable ties holding it.
- Check if there are no mounting brackets overlapping.

### **5.3.7 Cabling**

After all mechanically install on the boxes the cables are attached inside of each box and they need to be routed along the APA to the feedtrough position on the top of the detector. The cables will be attached to to APA for security and strain relief. It will be done using clamps made of PTFE and assembled with standoff screws as shown in figure

25, this clamps can be stacked making room for each layer of cables. On the top o the APA the cables will sit in the cable trays and be attached to it using cable ties and the excess cables will make a loop and be safely secured in APA for the detector move. The cabling routing will be made for each set of two columns of box in a procedure is as follow.

Figure 25 – The cables being hold in place with the PTFE clamps



Source: Author (2023).

- Starting for the two box on the bottom of the column. Open the back covers and remove all the temporary cable ties inside the box. Gently move the cables outside the box by the cabling window (always check if the window have the edge protectors on it).
- Pull all cable for the two boxes and tie them together using cable ties forming a bundle of 16 cables and using tape and static proof bubble plastic protect the



connectors on the end.

- Attach the cable bundle on the APA using a set of standoff and clips in the first level, use cable ties to secure the bundle to the clip.
- repeat from the second level to the last using stackable standoffs until reach the cables tray.
- Lay the cables in the cable trays attaching to it using cable ties until reach the feedtrough position.
- keep looping the cables in the same cable tray until it is all secured. Pay extra attention to secure the connectors.
- repeat the procedure for the second and third level boxes, using the final clips on the standoffs for each level.
- When all the cables are in place use cable ties to secure them together with cable ties to make extra strain relief.
- Assembly the back covers in all the boxes.

### 5.3.8 Quality control

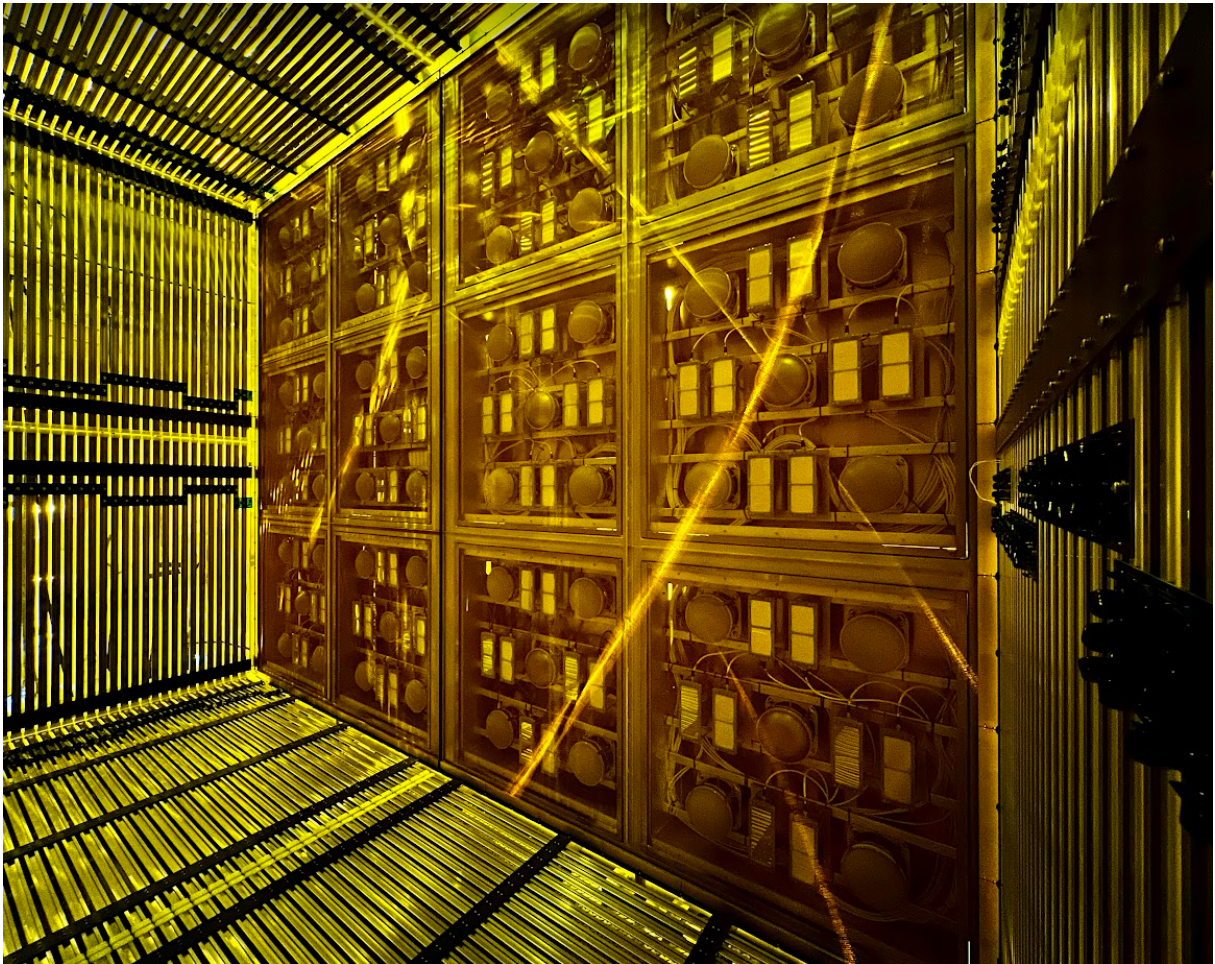
When all cables are done, some tests may be done to check if there haven't happen any damages on the cables or devices during the procedure. The testes are as following:

- Using the test board check all the grounding pins on the RJ45 connector in respect to the APA ground looking for any ground loop caused by a broken cable.
- Check the same for the grounding on the shielding cover on the cables that are in contact to the metal cover on the RJ45 connector.
- Check the nominal resistance and the low light tension expected in each channel of the X-ARAPUCA cables. Check the cable number to ensure the correct electrical diagram of the tested cable.
- Visually inspect the RJ45 cables to ensure none is break.
- Check if the cables don't move in the trays, and they are not touching sharp edges on the sides of APA and trays.

## 6 FINAL THOUGHTS

The outcomes of our efforts manifest in the successful installation and fortification of the system within the detectors. Every X-Arapuca was meticulously installed, subjected to rigorous checks, and confirmed operational in both APA configurations, as visually documented in Figure 26. Furthermore, all cables were not only securely positioned but also meticulously prepared for relocation, as show in Figure 27. The connectors underwent thorough testing, ensuring their safety and functionality. Finally, protective covers were judiciously placed to safeguard the entire system during the impending move (Figure 28).

Figure 26 – An internal view of the PDS system installed in the west APA with the back covers in. All X-Arapucas and PMT's can be seen behind the wire planes.



Source: Author (2023).

Figure 27 – Views of the PDS cables sitting in tray and routed along the APA



Source: Author (2023).

Figure 28 – The detector with all dark covers during the move procedure



Source: Author (2023).

## REFERENCES

- 1 HATSUMI, M. **The art of life and death**: Lessons in budo from a ninja master. Tokyo: Tuttle Publishing, 2012. ISBN 978-1-4629-0995-7.
- 2 BOTOGOSKE, G. **Aplicação da tecnologia Arapuca para detecção de luz de cintilação em argônio líquido e radiação Cherenkov em água**. 2023. (Master in Physics) - Universidade Estadual de Campinas, Campinas, SP, 2023.
- 3 AGUILAR-AREVALO, A. Updated MiniBooNE neutrino oscillation results with increased data and new background studies. **Physical Review D**, American Physical Society (APS), v. 103, n. 5, Mar. 2021.
- 4 THOMSON, M. **Modern Particle Physics**. New York: Cambridge University Press, 2013. ISBN 978-1107034266.
- 5 ARAUJO, G. **Wavelength Shifting and Photon Detection of Scintillation Light from Liquid Argon**. 2019. (Phd in Physics) - University of Zurich, Zurich, CH, 2019.
- 6 SEGRETO, E. Properties of liquid argon scintillation light emission. **Physical Review D**, American Physical Society (APS), v. 103, n. 4, fev. 2021. ISSN 2470-0029.
- 7 AGUILAR, A. *et al.*. Evidence for Neutrino Oscillations from the Observation of Electron Anti-neutrinos in a Muon Anti-Neutrino Beam. **Phys. Rev. D**, v. 64, n. 11, p. 112007, Nov. 2001. ISSN 0556-2821, 1089-4918.
- 8 DENTLER, M. *et al.* Updated global analysis of neutrino oscillations in the presence of eV-scale sterile neutrinos. . **J. High Energ. Phys.**, v. 2018, n. 8, p. 10, 2018. ISSN 1029-8479.
- 9 ARIAZZO, S. *et al.* Updated Global 3+1 Analysis of Short-BaseLine Neutrino Oscillations. **J. High Energ. Phys.**, v. 2017, n. 6, p. 135, June 2017. ISSN 1029-8479.
- 10 MACHADO, A. A. *et al.* The X-ARAPUCA: An improvement of the ARAPUCA device. **Journal of Instrumentation**, 2018.
- 11 WORKMAN, R. L. Review of Particle Physics. **PTEP**, v. 2022, p. 083C01, 2022.
- 12 ICECUBE. All about neutrinos. **IceCube Neutrino Observatory**, 2013. Available at: <<http://icecube.wisc.edu/info/neutrinos>> . Accessed: 21 Jan. 2024.
- 13 BROWN, L. M. The idea of the neutrino. **Physics Today**, v. 31, n. 9, p. 23–28, 09 1978. ISSN 0031-9228.
- 14 PAULI, W. Dear radioactive ladies and gentlemen. **Physics Today**, 1978.
- 15 STENICO, G. V. **Neutrino phenomenology in Short-baseline experimentstst**. 2021. (PhD in Physics) - Universidade Estadual de Campinas, Campinas, SP, 2021.
- 16 REINES, F.; COWAN, C. L. Detection of the Free Neutrino. **Phys. Rev.**, American Physical Society, v. 92, p. 830–831, Nov. 1953.

- 17 DANBY, G. *et al.* Observation of High-Energy Neutrino Reactions and the Existence of Two Kinds of Neutrinos. **Phys. Rev. Lett.**, American Physical Society, v. 9, p. 36–44, July 1962.
- 18 PONTECORVO, B. Mesonium and antimesonium. **Soviet Phys. JETP**, 2 1958.
- 19 PONTECORVO, B. . Neutrino Experiments and the Problem of Conservation of Leptonic Charge. **Zh. Eksp. Teor. Fiz.**, v. 53, p. 1717–1725, 1967.
- 20 CLEVELAND, B. T. *et al.* Measurement of the Solar Electron Neutrino Flux with the Homestake Chlorine Detector. **The Astrophysical Journal**, v. 496, n. 1, p. 505, Mar. 1998.
- 21 AHMAD, Q. R. Direct Evidence for Neutrino Flavor Transformation from Neutral-Current Interactions in the Sudbury Neutrino Observatory. **Phys. Rev. Lett.**, American Physical Society, v. 89, p. 011301, June 2002.
- 22 AGUILAR, A. Evidence for neutrino oscillations from the observation of anti neutrinos electronic appearance in a anti neutrinos muonic beam. **Physical Review D**, American Physical Society (APS), v. 64, n. 11, Nov. 2001.
- 23 BARREIROS, D. M. **A Minimal Seesaw Model for Neutrino Masses and the Origin of Matter**. 2017. (Master in Physics) - Universidade de Lisboa, Lisboa, PT, 2017.
- 24 WURM, M.; FEILITZSCH, F. von; LANFRANCHI, J.-C. **Neutrino detectors handbook of particle detection and imaging**. [S.l.]: Springer International Publishing, 2021.
- 25 Fermi National Accelerator Laboratory. **All things neutrinos**. 2023. Available at: <<https://neutrinos.fnal.gov/>> . Accessed: 01 May 2023.
- 26 HILKE, H. J. Time Projection Chambers. **Rep. Prog. Phys.**, v. 73, n. 11, p. 116201, 2010.
- 27 RUBBIA, C. The Liquid Argon Time Projection Chamber: A New Concept for Neutrino Detectors. **Ep Internal report**, p. 77–08, 1977.
- 28 NYGREN, D. (Ed.). **1974 PEP summer study**. [S.l.: s.n.], 1974.
- 29 CHARPAK, G.; RAHM, D.; STEINER, H. Some developments in the operation of multiwire proportional chambers. **Nucl. Instrum. Methods** **80**, 1 1970.
- 30 BORGHESANI, A. F.; LAMP, P. Electron Mobility in Dense Argon Gas at Several Temperatures. **Dielectrics and Electrical Insulation, IEEE Transactions On**, 2002.
- 31 YANG, T. Calibration of Calorimetric Measurement in a Liquid Argon Time Projection Chamber. **Instruments**, MDPI AG, v. 5, n. 1, p. 2, dez. 2020. ISSN 2410-390X.
- 32 MIYAJIMA, M.; TAKAHASHI, T.; KONNO, S.; HAMADA, T. Average energy expended per ion pair in liquid argon. **Phys. Rev. A**, American Physical Society, v. 9, p. 1438–1443, Mar. 1974.

- 33 SEGRETO, E. **TPC detection technology for neutrinos and dark matter:** School and workshop on dark matter and neutrino detection. 2018. Available at: <https://www.ictp-saifr.org/school-on-dark-matter-and-neutrino-detection/> . Accessed: 03 Dec. 2023.
- 34 CRESPO-ANADON, J. I. Status of the Short-Baseline Near Detector at Fermilab. **J. Phys.: Conf. Ser.**, v. 2156, n. 1, p. 012148, dez. 2021. ISSN 1742-6596. Publisher: IOP Publishing.
- 35 MACHADO, P. A. N.; PALAMARA, O.; SCHMITZ, D. W. The Short-Baseline Neutrino Program at Fermilab. **Annu. Rev. Nucl. Part. Sci.**, v. 69, n. 1, p. 363–387, out. 2019. ISSN 0163-8998, 1545-4134.
- 36 COLLABORATION, D.; ABI, B.; ACCIARRI, R.; ACERO, M. A. Long-baseline neutrino oscillation physics potential of the DUNE experiment. **Eur. Phys. J. C**, v. 80, n. 10, p. 978, out. 2020. ISSN 1434-6044, 1434-6052.
- 37 BERTUZZO, E.; JANA, S.; MACHADO, P. A. N.; FUNCHAL, R. Z. Dark neutrino portal to explain miniboone excess. **Phys. Rev. Lett.**, v. 121, n. 24, p. 241801, dez. 2018. ISSN 0031-9007, 1079-7114.
- 38 BALLETT, P.; PASCOLI, S.; ROSS-LONERGAN, M.  $U(1)'$  mediated decays of heavy sterile neutrinos in MiniBooNE. **Phys. Rev. D**, v. 99, n. 7, p. 071701, abr. 2019. ISSN 2470-0010, 2470-0029.
- 39 BATELL, B. *et al.* Inelastic dark matter at the fermilab short baseline neutrino program. **Phys. Rev. D**, v. 104, n. 7, p. 075026, out. 2021. ISSN 2470-0010, 2470-0029.
- 40 MAGILL, G. *et al.* Millicharged particles in neutrino experiments. **Phys. Rev. Lett.** v. 122, n. 7, p. 071801, fev. 2019. ISSN 0031-9007, 1079-7114.
- 41 MACHADO, A. A.; SEGRETO, E. ARAPUCA a new device for liquid argon scintillation light detection. . **J. Inst.**, v. 11, n. 02, p. C02004, fev. 2016. ISSN 1748-0221.
- 42 WHITTINGTON, D.; MUFSON, S.; HOWARD, B. Scintillation Light from Cosmic-Ray Muons in Liquid Argon. **J. Inst.**, v. 11, n. 05, p. P05016–P05016, maio 2016. ISSN 1748-0221.
- 43 DOKE, T. **Experimental Techniques in High-Energy Nuclear and Particle Physics**. 2. ed. [S.l.]: WORLD SCIENTIFIC, 1991.
- 44 PLASTICS, C. **Glass Epoxy Composite Material Properties and Uses as Flame Retardant**. Curbell Plastics, 2023. Available at: <https://www.curbellplastics.com/materials/plastics/g10-fr-4-glass-epoxy/> . Accessed: 09 Jan. 2024.